Potential for PRO in the North of Mexico: Theoretical analysis of the feasibility based in the Area Power Output

EDUARDO JOEL LOPEZ-TORRES

Abstract

The global interest in renewable energies to substitute the fossil fuels has led to the development of new technologies and processes to obtain energy. The sources were the energy is obtained from vary, but when the resource is scarce this technologies need a different approach to make the process sustainable. In the cases of those related to water, PRO is an interesting process that could cover both requirements in places like the North of Mexico, were the amount of available water is low and the energy demand high. PRO consists in the controlled mixture of two solutions with a greater salinity were the pressurised high salinity one could be used to produce energy depressurizing it. In this work, the feasibility of implementing PRO technology in the North of Mexico is analysed. The salinities of Panuco, Soto La Marina and Mayo rivers are analysed to determine the points were the requirements for this process are fulfilled. Different reported membranes performances are compared and the best values values are tested using the information from the rivers and a modified formula for calculating water flux and area power output in PRO. The results show that analysed scenarios present a high potential for PRO applications, were under the situations analysed in this work they could reach an area power output over the minimal required to make the process feasible (5 W/m^2). However, it is still necessary to design a more suitable PRO plant and a way to obtain fresh water from a shorter distance.

Potential for PRO in the North of Mexico: Theoretical analysis of the feasibility based in the Area Power Output

Eduardo Joel Lopez Torres

This dissertation is submitted to obtain the degree of Msc in Engineering

Engineering Department

Durham University

2019

Table of Contents

Table of Figures

List of Abreviations

AL: Active Layer

AL-DS: Active layer facing the draw solution

AL-FS: Active layer facing the feed solution

CNA: Comision Nacional del Agua (National Water Comission)

CTA: Cellulose Triacetate

DS: Draw Solution

FS: Feed Solution

ODMPs: Osmotically-driven Membrane Processes

PRO: Pressure Retarded Osmosis

RED: Reverse Electrodialysis

SENER: Secretaria de Energia (Secretariat of Energy)

SL: Support Layer

TFC: Thin Film Composite

List of symbols

J_w	Water flux, LMH
W	Area Power Output, W/m2
$\Delta\pi$	Osmotic pressure difference across the membrane, bar
π_{fs}	Osmotic pressure of the Feed Solution, bar
π_{ds}	Osmotic pressure of the Draw Solution, bar
ΔP	Hydrostatic pressure difference across the membrane, bar
A	Water permeation coefficient, LMH/bar
B	Solute permeability coefficient, LMH
k_c	Mass transfer of the channel adjacent to the active layer, µm/s
k_{sup}	Mass transfer coefficient of the support layer and its adjacent external channel, µm/s

Statement of Copyright

Acknowledgments

Thanks to my mother who has been always supporting my ideas, no matter how unconventional they are. To Enrique Vargas who believed, and still believes, in me and helped me with the whole process of coming to United Kingdom. To Jack Francis who has help me to cope with my most stressful moments during my time here.

Thanks to Dr Teresa Alonso, Laura Sinagawa and teacher Arrambi who, without a doubt, were an important support before coming to United Kingdom. Also to the Universidad Tecnologica de Altamira for giving me the opportunity to study such an interesting topic that could be beneficial for our country.

Thanks to my supervisor Professor Jun Jie Wu, who has been very supporting in a professional and personal way and without her I wouldn't be able to fulfil my studies. Also thanks to Robert Field who helped me to understand better such a complex topic. To Christine and Ian for their technical support during some of the stages of my experimentation.

To my friends and family, for giving me the necessary support during my time abroad. I could write an extensive list of people I would love to thank for but it will take me more than one page. But I want to especially thank Trishla Singh for helping to understand myself in my deepest moments and keep my in track with my work. Charles Walker and Dominic Birch for teaching me that life is not only work and the best way to keep going and make a brighter future is being ourselves. Alastair Stewart for giving me advice of how to balance my professional and personal life. Oscar Ochoa, Marcos Cruz and Maura Ramirez for taking me under their wing and provide me with a tremendous amount of support of all kind. Thanks to my Mexican friends Hiram, Oscar, Emilio, Gerardo, Brian, Alejandro, Juan Carlos, Emmanuel, Julio and Leopoldo who were my family away from home. Thanks to Stuart Foster, my college mentor, who did an amazing job making me feel comfortable and adapt to the British Culture. Thanks to Nestor Torres, who even with the time differences he always keeps in touch with me and makes me feel that I still have a place to go back once I'm in Mexico. Thanks to Joseph Schenkel for making my time at the Fencing Club the best I could ever have and impulse my curiosity for such an interesting sport. And the list could go on but I'm running out of space.

Thanks to CONACYT-SENER for providing me with the funds to pursue this major under the scholarship No. 495379.

Thanks to Durham University for providing me with the facilities and resources required to fulfil my major.

And last but not least, thanks to the Higher Power (Whatever that is) for providing me with an amazing experience in a professional and personal level that broad my perspective of the World and, for sure, will mark my life.

Dedication

To the people in my country who are fighting for a better future. Never give up, we are all together on this and we will succeed.

Chapter 1. Introduction, Aims and Objectives

1.1. Introduction

There has been a growing worldwide interest in renewable energies as a substitute for other common energy sources, especially fossil fuels. The main reasons for the transition between fossil fuels and renewable energy sources is the desire to decrease pollution and develop more sustainable energy production. In order to achieve these goals, a change in energy policies and practices is required.

Table 1. National Energy Balance: Primary Energy Production in Petajoules. Adapted from: Sistema de Información Energética, SENER [1].

Primary Source	Year			
	2014	2015	2016	2017
Carbon	**303.73**	**287.69**	**254.17**	**308.24**
Hydrocarbons	**7782.96**	**7203.85**	**6694.85**	**5940.6**
- Crude Oil	5597.2	5067.69	4826.85	4354.89
- Condensed	106.31	98.83	88.31	67.28
- Natural Gas	2079.45	2037.32	1779.68	1518.43
Nuclear Energy	**100.6**	**120.41**	**109.95**	**113.22**
Renewables	**666.97**	**649.09**	**655.16**	**665.16**
- Hydropower	140.01	111.21	110.51	114.65
- Geoenergy	129.88	134.53	132.59	127.43
- Solar Energy	8.73	10.15	11.09	15.16
- Eolic Energy	23.13	31.48	37.36	38.23
- Biogas	1.93	1.87	1.91	2.52
Biomass	**363.28**	**359.84**	**361.7**	**367.18**
- Bagasse of cane	109.16	107	110.14	116.87
- Firewood	254.12	252.84	251.56	250.31
Total	**8854.25**	**8261.03**	**7714.13**	**7027.22**

The Mexican government has been working in the transition since 2015, with the publication of the Energy Transition Law [2]. The objective of this law is to regulate most of the issues related with Clean Energies, the sustainable usage of energy and reduce the pollution generated by the Energy Industry [2]. Moreover, it promotes the development of new technologies related to the generation, distribution and storage of energy from different sources [2]. The use of clean energies in Mexico had been explored before the implementation of this law, with examples such as the geothermal

plant Azufres III, the wind turbine park Los Altos and the photovoltaic central Aura Solar I [3]. As could be seen in *Table 1*, the proportion of energy from renewable sources is around 10% of the total production [1]. This demonstrates Mexico's current interest in the global goals of the transition to clean energy.

Due to the location of the country and its geography, Mexico has a strong potential for growth in the use of renewable energies, in particular water-based energy production. The territory is surrounded by two different oceans (Atlantic and Pacific), and also possess 51 main rivers that provide fresh water to the population [4]. However, the possibility of using water for energy production is limited by the distribution of water in different parts of the country. According to the National Water Commission (Comision Nacional del Agua, CNA), the Southeast region of Mexico possess two thirds of the renewable water of the country, while the north and centre only possess one third of it. At the same time two thirds of the population live in the North while one third lives in the South [5]. This means that any possible use of the water in the North could shorten the supply of this resource. For this reason, water-driven energy production processes must consider the availability of fresh water.

Members of the CEMIE-Oceano, a multidisciplinary network of researchers and research centres in Mexico, published an article assessing the potential of ocean-related energy systems. They analysed the theoretical potential for wave energy, ocean currents, thermal gradient and salinity gradient in Mexico, obtaining optimistic results that encourage the development and implementation technologies of this kind [6]. The results shown on this article are theoretical results that acknowledge that the influence of energy recovery devices, environmental and socio-economic impact should be considered in further research. This is the first document of its kind focused on the country and gives an overview of the energy harvesting potential.

Specifically for salinity gradient energy, it is important to understand the nature of the process and variables involved to avoid a decrement in the energy production. One of the most studied procedures to harvest energy from the salinity gradients is the pressure Retarded Osmosis (PRO). PRO is a methodology based in the controlled mix of a solution with a low salinity (Feed Solution) and other with a high salinity (Draw Solution) that allow us to harvest energy using recovery devices [7] [8] [9] [10]. PRO could be combined with desalination and waste water treatment to generate fresh water

with a lower energy consumption [11], making the process more attractive for places where the availability of water is limited. Moreover, it is important to examine real water bodies when assessing the feasibility of a PRO plant [12]. In 2002 S. Loeb suggested a methodology to calculate the feasibility of PRO plants under different conditions using real water bodies as a base [12]. Although those are still used as a base for PRO projects, some of the values and formulas require updating.

1.2. Aims and Objectives

1.2.1. General Objective

Analyse the feasibility of implementing PRO systems in the North of Mexico using a modified version of the analysis proposed by Loeb [12] that considers the latest understandings of mass transfer in membrane science.

1.2.2. Specific Objectives

- Establish the operational conditions based on the salinity of three Mexican estuarine systems in the North of Mexico.

- Classify membranes reported in the literature according to their material composition and analyse their performance for PRO systems.

- Calculate the possible Water Flux (J_w) and Area Power Output (W) of the membranes showing performance under the chosen operational conditions.

- Analyse if the Area Power Output obtained from those calculations is enough to fulfil the minimum required, established in [13].

Chapter 2. Literature Review

2.1. Hydrological situation in Mexico

Every year, CNA reports the state of the water resources in Mexico in a document called “Statistics on Water in Mexico”. This report analyses the topic with indicators related to quality, demography, meteorology and economics. For management reasons, CNA divides the water resources in 13 basin councils known as the Hydrological-administrative regions (HARs). Mexico counts 51 rivers, of which 33 disembogue at the Pacific Ocean or Gulf of California, and 16 the Gulf of Mexico and Caribbean Sea. In total it has 757 watersheds for the management of surface water and 653 aquifers for groundwater management [4]. In 2017, $2.7x10^{11}$ m^3 were allocated for the consumption in urban or domestic use, from which 8.7 $x10^{11}$ m^3 were designated as consumptive water and 1.8 $x10^{11}$ m^3 for non-consumptive purposes. 90.4% of the consumptive water was designated for agriculture and public supply, 4.9% for industrial usage and 4.7% for electricity generation (Not including hydropower), while 99.99% of the non-consumptive water was destined for hydropower generation [14]. From the allocated water for hydropower, only $1.3x10^{11}$ m^3 (73.16%) was actually employed. With that amount, it was possible to generate 30.1 TWh of electricity, corresponding to 11.7% of the national total [14].

The 9 HARs corresponding to the North, Central and North West area of the country possess one third of the total renewable water. As mentioned before, those areas count with most of the population and provide a high percent of Gross Domestic Product of the country [14]. The water stress in Mexico is low considering it as a whole, but furtherly analysing the HARs, all of them are considered to have a “High” stress [14]. The scarcity of water in those places can be attributed to environmental factors (i.e. the biomes present on those regions, weather conditions, and geography), demographics and overexploitation of the resource.

There are 5028 monitoring sites for water quality of which 3910 are focused on surface water and coastal areas. The main three monitored parameters are biological and chemical oxygen demand, total suspended solids and faecal coliforms [14], each of them has to be done fulfilling the requirements established by different Mexican regulations. The parameters and methodologies covered by those regulations

comprehend a wide variety of analytes, which can be determined in different water matrixes.

2.2. Salinity Gradient

Knowing the hydrological situation of Mexico it can be said that the potential for water-based energy production processes is relatively high [6]. Considering that Mexico is surrounded by two oceans the idea of using them as a water source for those processes is attractive as it won't deplete the availability of the fresh water. The ocean energy can be harvested through wave motions, marine currents, thermal gradients and salinity gradients. However, most of the harvesting methods could impact drastically on the ecosystem. Methodology to counteract this possible impact must be considered in the development of those technologies.

From the mentioned methodologies, salinity gradient possess two advantages over the rest. The first one is that it happens naturally in places like estuarine systems where river water and seawater mixes, only requiring methods to "control" this mixture. The second is that the resulting secondary products (Water with a different concentration from the original sources) could be easily treated in order to diminish the possible impact of discharging them back to the original water bodies or use them in other processes. The two main studied salinity gradient energy production processes are Reverse Electrodialysis (RED) and PRO. Whilst RED requires the usage of specific ions in the water with affinity to the electrodes used to obtain the energy [15], PRO exploits the osmotic pressures of both solutions making the pre-treatment less complex and, therefore, decreasing the possible cost of energy production.

The osmotic pressure (π) of any solution depends mainly of the dissolved solutes and their interactions with the solvent [16] [17]. In his research, Loeb uses specific values for the river water and seawater osmotic pressures. Loeb considered an osmotic pressure of 25 bar [12], which is similar to what was previously suggested as an "ideal solution" of sea water (26.7 bar) [16]. The average salinity of the Seawater is of 35‰ and its composition could be seen in *Table 2*.

Table 2. Average concentrations of the major ions in seawater, in parts per thousand by weight (g kg-1 or g l-1). Retrieved from 'Seawater: its composition, properties and behaviour', by Brown, E. et al [18].

Ion	‰ by weight
Chloride, Cl-	18.98
Sulphate, SO42-	2.649
Bicarbonate, HCO32-	0.14
Bromide, Br-	0.065
Borate, H2BO3-	0.026
Fluoride, F-	0.001
Sodium, Na+	10.556
Magnesium, Mg2+	1.272
Calcium, Ca2+	0.4
Potassium, K+	0.38
Strontium, Sr2+	0.013
Overall total salinity	34.482

While the composition of the seawater remains similar across the world (with certain exceptions), the river water composition could be completely different. The composition of the surface water bodies would vary according to their natural runoff (where the river passes through) and usage of the same for different activities [18] [19].

As mentioned before, PRO benefits from the mixture of two solutions with different salinities, therefore, different osmotic pressures. The osmotic pressure difference ($\Delta\pi$) it's the difference between the high and low salinities osmotic pressure. Loeb considered Mississippi River osmotic pressure as 0 bar [12], which turns it into an ideal solution without any kind of solutes. In this case $\Delta\pi$ is of 25 bar which, ideally, should generate a great amount of power but in reality does not (this will be further discussed in section 2.3). Making assumptions about the osmotic pressure makes it easier to calculate the power output, but ignoring the real conditions of the water system doesn't allow for determining the suitability of a plant location.

2.3. Pressure Retarded Osmosis

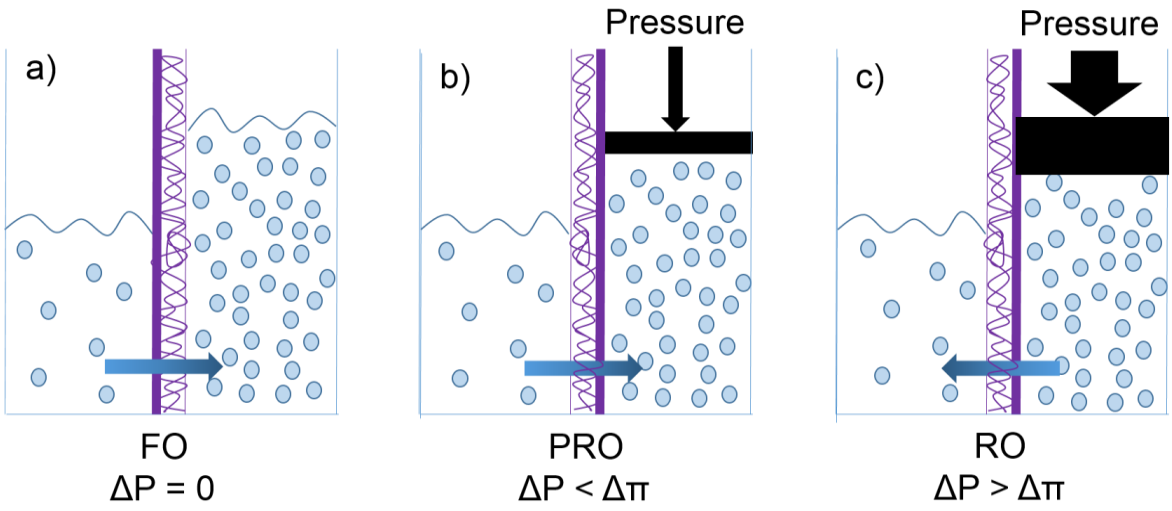

Figure 1. Mass transfer at different osmosis processes. In FO (a) the there is no exerted pressure over the draw solution (Right) so the feed solution flows through the membrane to the saturated side solely by osmosis. In PRO (b) and RO (c) the hydraulic pressure (ΔP) exerted over the draw side changes the flow. However in (b), ΔP is lower than the osmotic pressure difference (Δπ) and still allows the FS to cross the membrane. (c) Illustrates reverse osmosis. In this figure, the thick section of the membrane symbolizes the active layer of the membrane.

One of the main reasons PRO is interesting is the possibility to use it as sustainable and renewable energy production system. PRO consists in the controlled mixture of the Feed Solution (FS) and the Draw Solution (DS) using a membrane. The PRO mechanism could be considered a middle point between Forward Osmosis and Reverse Osmosis, as explained by Achilli (see *Figure 1*) [7]. The FS permeates through the membrane to the draw side due to the osmotic pressure difference across the membrane, pressurizing the draw solution. In order to control the flow of water, and to produce power, a pressure (hydraulic pressure) is exerted at the DS side. The hydraulic pressure should not exceed the value of osmotic pressure difference ($\Delta P < \Delta\pi$) and is typically 0.5 $\Delta\pi$. The energy is harvested from the pressurised water using Energy Recovery Devices or hydro-turbines and transformed into electricity [7] [8] [20] [21] [22].

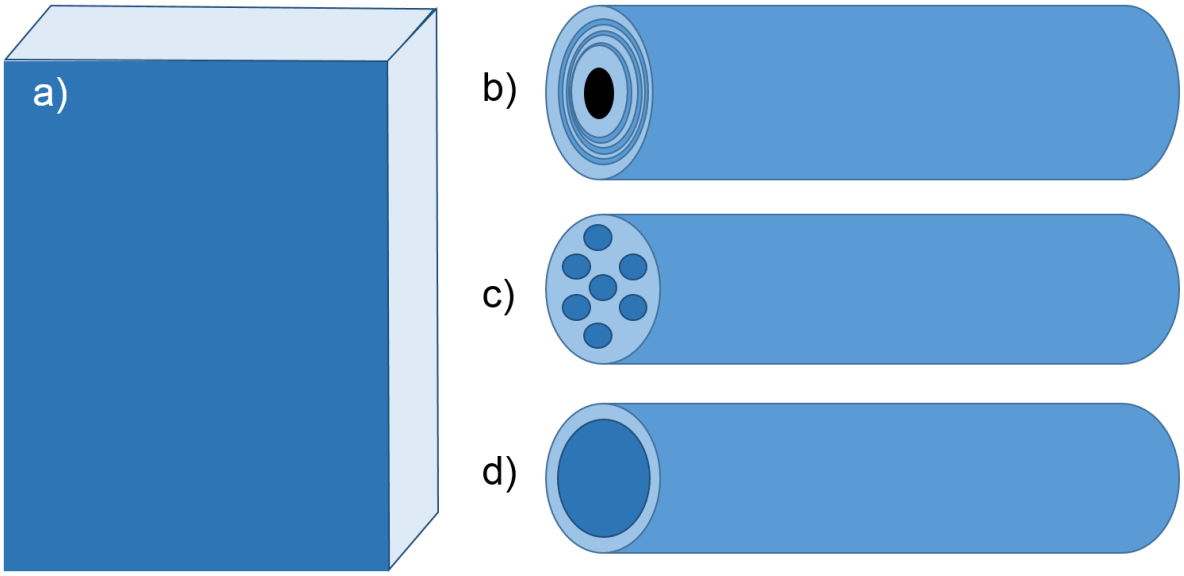

Figure 2. Different membrane modules. Flat sheet (a) are widely used in the industry. Spiral wounds (b) are made with different flat sheets around a collection tube. Hollow fibers (c and d) are tubular membrane; (c) is a multi-bore fiber.

The Osmotically-driven Membrane Processes (ODMPs) such as PRO depend mainly on the membrane properties. Membranes are developed in different shapes (modules). The two main types of membrane modules are Flat Sheets and Hollow Fibers [23] [24]. The first one could be completely flat (Flat Sheet) or wrapped around a central collection tube (Spiral Wound). The second one consists of a bundle of long porous tubes that are single or multi-bores (See *Figure 2*). Usually the membranes are made with Cellulose Triacetate (CTA) or a combination of a polymeric matrix with a thin layer of another material to enhance their properties (Thin Film Composite or TFC). Most of the membranes possess two different layers, a support layer (SL) and an active layer (AL). While the SL provides structure for the membrane, the AL rejects the solutes controlling what passes from one side to another. The morphology of those layers and the module shape affect the overall performance of the membrane.

Water permeability (*A*) and salt rejection (*B*) are two critical parameters affected by the membrane characteristics. Water permeability could be considered as a measure of the ability of the membrane to allow water to pass from one side to the other, while the salt rejection is the resistance of the membrane to allow salt through the membrane. *A* and *B* are key values in ODMPs because they determine the overall performance of the membrane. The performance is also affected by the nature of the solutions

employed and the flow orientation due the Concentration Polarization [7], which will be discussed later in this section.

The water flux (J_w) is the most relevant variable for ODMPs, especially for PRO. *Equation (1)* shows the basic way to calculate the water flux.

$$Jw = A\ (\Delta\pi - \ \Delta P) \quad (1)$$

Where $\Delta\pi$ and ΔP are the osmotic and hydraulic pressure differential across the active layer of the membrane. J_w specifies the rate at which a volume of water flows across the membrane. However, this equation does not consider the effects of Concentration Polarization during the osmotic process making it inaccurate.

The importance of J_w lies in its relation with the power output (W) of the system, as could be seen in *Equation (2)***.**

$$W = Jw \cdot \Delta P \quad (2)$$

If we substitute *Eq. (1)* in *Eq. (2)* we will obtain equation *Eq. (3)*. Considering the nature of the osmotic processes, if the value for ΔP is equal to 0 or $\Delta\pi$ the power output would be equal to 0. However, if we consider $\Delta P = \frac{\Delta\pi}{2}$ then the power output would reach its highest value, as could be seen in *Figure 3*.

$$W = \ A\ (\Delta\pi - \ \Delta P)\ \Delta P \qquad (3)$$

In 2002, S. Loeb published an article analysing a PRO system that would harvest energy from the Mississippi River and the Gulf of Mexico [12]. The article focused on determining the feasibility of a PRO plant under specific conditions. The calculations were done considering a hypothetical plant with the same specifications as Yuma RO plant (Arizona, US) to calculate things like costs and power output of the PRO plant. The Mississippi River was considered the FS while the Gulf of Mexico the DS, making it comparable to other combinations of River water/Seawater systems. The article also includes a possible arrangement for the PRO process equipment which its energy consumption is considered at the power calculations as a loss, trying to make it sustainable. Combining both technical and economic information the article shows an attractive way to develop projects of this kind.

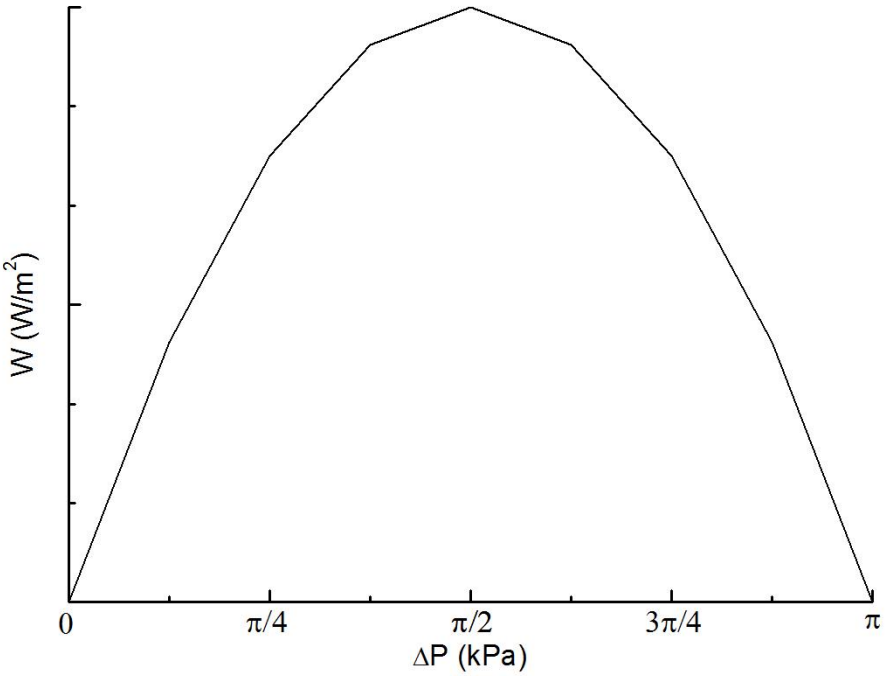

Figure 3. Schematic diagram showing the behaviour of W at different values of ΔP. The highest energy value obtainable from the hydraulic pressure would be, for an ideal system, half the value of the osmotic pressure.

Table 3. Adaptation of the "Technical summary" table from [12] and the original values employed in the calculation. For technical purposes, the values for the permeate rate, area per element, elements per module and net power were set as the plant operational conditions in the calculations done in this document.

	Description (Units)	Value
A	Permeate Flux (m^3/m^2*d)	0.29
B	Permeated Rate (m^3/d)	2000000
C	Area per element (m^2/element)	117
D	Elements per module (element/module)	3
E	Net Power (kW)	22300
F	Membrane Life (y)	7
G	Operating days (d)	330
H	Hours per day (h/d)	24
I	Total Membrane Area (m^2) (B/A)	6896551.72
J	Number of modules required (I/(C*D))	19648.3
K	Modular Power (kW/module) (E/J)	1.13
L	Area Power (kW/m^2) (E/I)	0
M	Area Energy (kWh/m^2) (L*F*G*H)	179.27
N	Area Power in W/m^2	3.23

While at lab scale the obtained results could be promising, at in-plant conditions this is likely to be different. Loeb's calculations considered those differences as part of its "technical summary" for the PRO plant, obtaining the power density (*W*) of the system under specific conditions and the theoretical total energy generated by the membrane during its lifetime [12] (See *Table 3*). Even if the plant specifications change (i.e. the number of modules used, their total area, water flow, etc.) the formula would give an overview of the power production.

Most of the variables used in the article were "optimistic assumptions" that, as previously mentioned, make the PRO projects attractive but not realistic. Moreover, the theories relating to mass transfer in osmotically driven processes, water properties and their relation with PRO energy production have developed over time. Since then, several studies were developed to determine the feasibility of this option, but as explained in [9], the viability of the process is still not reachable with the current commercially available membranes. In order to achieve it the average power output of those systems should be over 5W/m^2 [13].

As mentioned before, another problem in ODMPs is the Concentration Polarization. This effect could change the concentration of the solution near the membrane surface and induce a decrement in the water flux or promote fouling [25]. Concentration Polarization has two main variants: Internal and External. The first occurs in the interior of the membrane structure while the second could happen at both surfaces in contact with the solutions. Both effects differ according to the membrane configuration (Active layer facing the draw solution (AL-DS) or the feed solution (AL-FS)). As in PRO processes the configuration should be AL-DS, the formula employed for this project would be as follows (*Eq. (4)* [25]).

$$Jw = K_{overall}\, ln\left[\frac{\pi_{ds}+\frac{B}{A}\left(1+\frac{A\Delta P}{J_w}\right)-\frac{J_w}{A}\left(1+\frac{A\Delta P}{J_w}\right)exp\left(\frac{J_w}{k_{ecp,al}}\right)}{\pi_{fs}+\frac{B}{A}\left(1+\frac{A\Delta P}{J_w}\right)}\right] \qquad (4)$$

Where J_w is the permeation rate of the water; $K_{overall}$ the overall mass transfer coefficient; *A* the water permeability of the membrane; *B* solute permeability coefficient; π_{ds} *and* π_{fs} the osmotic pressures of the DS and the FS respectively; ΔP the difference between the π_{ds} *and* π_{fs}; and $k_{ecp,al}$ the mass transfer coefficient near the active layer surface.

While most of the variables could be calculated with experimental data, $K_{overall}$ needs to be calculated as follows (*Eq. (5)* [25]):

$$\frac{1}{K_{overall}} = \frac{1}{k_{icp}} + \frac{1}{k_{ecp,sl}} + \frac{1}{k_{ecp,al}} \qquad (5)$$

Where k_{icp} stands for the mass transfer within the support layer; and $k_{ecp,sl}$ mass transfer near the surface of the same. As suggested by my supervisor, Professor Wu, a modified equation has been proposed and ΔP was introduced here [26]. The modified equation is as follows, and this equation has been used for the calculation of the effect of salinity:

$$J_w = A\left[\pi_{ds} exp\left(-\frac{J_w}{k_c}\right) - \pi_{fs} exp\left(\frac{J_w}{k_{sup}}\right) - \Delta P\right] + B\left(1 + \frac{A\Delta P}{J_w}\right)\left[exp\left(-\frac{J_w}{k_c}\right) - exp\left(\frac{J_w}{k_{sup}}\right)\right] \quad (6)$$

Where k_c corresponds to the mass transfer of the channel adjacent to the active layer and k_{sup} the support layer and its adjacent external channel.

Using *Eq. (6)* as the formula for the water flux calculation would be more accurate than the original calculations. However, it involves the introduction of new variables that were not considered before (k_c and k_{sup}). According to [27], the calculation of the mass transfer coefficient is as follows.

$$\frac{1}{k_{sup}} = \frac{1}{k_c} + \frac{S}{D} \quad (7)$$

Where S is the structural parameter of the membrane (Product of the support layer thickness and tortuosity over its porosity) and D the diffusivity of salt in water.

Equation (7) requires three different values to calculate k_{sup} of the system. Previous researches already obtained values for D under specific concentrations of certain solutes, especially sodium chloride [28] [29], making easy to perform the calculation if the molarity of the solution is known. S can be calculated after some experiments using the water flux equation as a base when the rest of the variables are known [21] [20] [30] [31]. k_c is determined by experimental measurements but, as the proposed methodology to calculate J_w is relatively new, there is little information regarding this value. Therefore, analysing the relationship between k_c and J_w is fundamental in order to improve PRO systems.

So far, there are only two pilot cases where PRO was used as a possible system to harvest energy: Statkraft in Norway [13] and “Mega-Ton Water System” in Japan [11]

[32]. The first case was cancelled due to poor performance of the membrane [11] [13], which did not reach the 5 W/m^2 power output. The second case was designed as a seawater desalination plant (SWRO) where a PRO system was included to reduce the energy consumption [11]. The average of the power output was of 13.3 W/m^2, which is almost three times the required energy to consider it feasible. The key for the success of the PRO system at Mega-Ton is the combination between a controlled desalination system to avoid the fouling of the membranes and the technologies developed for that project [11] including a novel membrane.

The water flux calculation should be updated to one that considers the membrane properties (such as water permeability and salt rejection) and the latest understanding in mass transfer related effects. In this project we will use the values given in [27] and the diffusivity values provided by [28]and [29] as a reference to calculate k_{sup} and J_w under specific scenarios.

Chapter 3. Methodology and Source of Data

3.1. River water-Seawater Scenarios

Information related to the different rivers in the North of Mexico that disembogue at the sea was requested to the CNA. Such information included the location of sampling points across the whole river length and the salinity at those points from 2015 to 2017 (See Appendix 1). A mean of those values was calculated and then analysed. Considering the location of all the sampling points, those rivers with enough information were chosen to continue with the analysis.

Sampling points with a similar distance (Around 50 km away from each other) and great salinity difference were chosen from each system.

Molarity was calculated using the values for the salinity of the chosen sampling points and the standard equation for molarity. In the cases where the salinity was not provided ([27] and [12]), it was calculated using the following formula:

$$Salinity\ \left(\frac{g}{kg}\right) = \frac{W}{W_{H2O}} \quad (8)$$

Where W is the weight of the solute employed to calculate the molarity in 100L of water and W_{H2O} is the water density multiplied by the same volume. With the salinity the Osmotic Pressure (π) was calculated interpolating their average salinity values with those in the MIT Seawater Thermophysical Properties Library [33] [34]. For practical purposes NaCl was considered as the only solute dissolved in those water bodies.

Diffusivity was obtained from [28] and [29]using the molarity as a reference. In the cases where the molarity was 0 the diffusivity was restricted by Nernst limiting values (See Appendix 2).

3.2. Water flux and theoretical power output

Six different salinity scenarios were analysed including the three estuarine systems, two lab scale salinities [27] and Loeb's original case [12]. Different arrangements were made to calculate the water flux of each membrane under each scenario. For k_c, the employed values were 10, 14.1 and 50 μm/s, the second corresponding to the value obtained from a commercial membrane [27] and the rest were selected to analyse the fluctuation in the results with a low (10 μm/s) or high (50 μm/s) mass transfer coefficient. The diffusivity coefficient of the FS was used along the mentioned k_c values to calculate k_{sup} (See Appendix 2 for further information).

For *A* and *B*, the performance of different membranes reported in the literature [20] [21] [27] [35] [36] [37] [38] [39] [40] [30] [41] [42] [43] [44] was compared against those reported in [12]. The membranes were classified according to their composition and then their performances compared. Those with the better performances were used for the water flux estimation using the previously calculated k_{sup} and π values for each scenario, and *Eq. (6)*.

The formula for J_w was used first under the *A* and *B* values reported in [27], then under those reported by [12], and finally against those of the chosen membranes. While the first calculations include the three values for k_c, the other two do not as it is an intrinsic property of that reported membrane. Therefore, the other two systems only consider k_c=10 and 50 μm/s. In all three cases, all the estuarine systems and Field's salinities were employed.

For the area power output (*W*), the calculation was realised under the plant specifications given in [12] as shown in *Table 3*. The results were organised following the same structure as for the water flux and compared against the goal of 5 W/m^2.

Chapter 4. Results and Discussion

4.1. Salinity Effects

To determine if a PRO power plant like the one proposed by Loeb could be feasible or not at any point of the world, an analysis of the salinity gradient of the water bodies system is required. For this specific research, the analysis was focused on three different river-sea systems located in the North of Mexico. The first system is the Mayo River (See *Figure 4*), located in the state of Sonora, and its river mouth at the Gulf of California (Pacific Ocean). The other two systems are Panuco River (*Figure 5*) and Soto La Marina River (*Figure 6*), both located in the state of Tamaulipas, and have their river mouths in the Gulf of Mexico (Atlantic Ocean). The average natural runoff and lengths of the rivers are given in *Table 4*.

Table 4. Comparison between Mexican rivers and Mississippi river.

River	River length (km)	Average Natural Surface Runoff (m^3/day)
Mayo [4]	386	$(3.30)(10^6)$
Panuco [4]	510	$(55.4)(10^6)$
Soto La Marina [4]	416	$(4.99)(10^6)$
***Mississippi* [12]**	3778	$(1500)(10^6)$

Figure 4. Mayo River Sampling points. The Mayo River flows through the state of Sonora until it reaches the Gulf of California.

Figure 5. Panuco River sampling points. The Panuco River flows through the states of Veracruz and Tamaulipas. Its river mouth is located at the Gulf of Mexico.

Figure 6. Soto La Marina River sampling points. This river flows through the state of Tamaulipas and disembogue into the Gulf of Mexico.

The data provided by the CNA comprises values since the beginning of 2015 until near the end of 2017 (See Appendix 1). The sampling points at each river were located at different distances from the river mouth, which helps to understand how the water properties change through the river length. One of the properties that changes drastically is the salinity. The river drags solids and salt from the different terrains that it flows through, until it reaches a point near the sea, ending with a salinity similar to the sea salinity. As the data provided did not include any specific sea water analysis, the nearest point to the sea was considered as the "Sea Side" (*M1*, *P1* and *S1*) and the distance was calculated with Google Earth Pro ©, using the natural river path as a reference for the sampling points order. The measurements were made by drawing a straight line from one point to the next one, starting with the "Sea Side" point, and adding the distance to the previous measurement. That way it is possible to understand how far away the fresh water source is from the sea (See *Table 5)*.

The water properties will vary according to the temperature of the water bodies [16] [17] and the different dissolved compounds [16] [17] [45], making it difficult to calculate the osmotic pressure with realistic values. Even if it is possible to obtain a specific water composition (i.e. metals [46], hardness [47], dissolved solids [48], etc.) or the temperature at the sampling point [49], those values will change with the pass of time. For this reason, it was decided to settle specific conditions for the pressure calculations.

It was considered that the water composition in all the analysed rivers was similar to the sea water composition, making easier to compare against the MIT Seawater Thermophysical Properties Library [33] [34]. As most of the Mexican water quality analysis use a deionized water sample blank at 25°C [46] [47] [48] the osmotic pressure was calculated under that specific temperature, interpolating the salinity values to those shown in [33] [34] obtaining the results shown in *Table 5.*

Loeb's analysis require two values with a high pressure difference, in other words a solution with a high salinity (Sea Water) and one with a low salinity (River Water). The salinities for Soto La Marina and Panuco River do not include values under 0.1 ‰, for this reason the lowest values (S6 and P9, respectively) were considered as the FS. In the case of Mayo River, M4 was chosen as the lowest value because the decrement ratio of the salinity at M5 is much lower than at M4. The proximity of M5 and M6 to the lagoon (see *Figure 4*) could affect the salinity properties of those sampling points.

Table 5. Average salinities and linear distance of each sampling point.

Sampling Point	Av Salinity (‰ or g/kg)	Linear Distance (km)	Osmotic Pressure (bar)
M1	36.3554	-	26.97
M2	0.3156	47.5	0.23
M3	0.1517	55.93	0.11
M4	0.1063	64.93	0.08
M5	0.0847	82.86	0.06
M6	0.0977	100.89	0.07
M7	0.1067	117.45	0.08
M8	0.1078	120.56	0.08
P1	34.1592	-	25.26
P2	19.0022	4.4	13.76
P3	17.6944	7.59	12.8
P4	17.4687	9.3	12.63
P5	16.9778	11.74	12.27
P6	5.1693	18.02	3.7
P7	0.8243	31.13	0.59
P8	0.4457	38.77	0.32
P9	0.2008	52.83	0.14
P10	0.2185	56.78	0.16
S1	35.8892	-	26.6
S2	31.723	0.35	23.36
S3	17.9013	48.34	12.95
S4	0.416	54.28	0.3
S5	0.4292	58.68	0.31
S6	0.33	78.39	0.24

4.2. Membrane Properties (*A* and *B*)

Since Loeb developed his calculations in 2002 [12] until this date, different kinds of membranes have been developed and their properties enhanced. According to his calculations, the possible improvements in water permeability, salt rejection and mass transfer of the membrane could affect directly the expected water flux and energy output. For this reason, an analysis of those properties is required.

Table 6. Water permeability (A) and salt rejection (B) of different membranes. In FO standard theory, the ratio of J_s and J_w is proportional to B/A. This table includes the material it is made of and the module type (FS for Flat Sheet, HF for Hollow Fiber).

	Membrane material	Module	A (LMH/bar)	B (LMH)	B/A (bar)
A [34]	CTA	FS	0.51	2.19	4.29
B [35]	CTA	FS	0.34	0.11	0.32
C [36]	TFC-CTA	FS	0.68	0.12	0.18
D [31]	CTA	FS	0.82	0.88	1.07
E [31]	CTA	FS	0.82	0.68	0.82
F [37]	CTA	HF	0.09	0.03	0.32
G [18]	TFC-PES	HF	3.8	0.44	0.12
H [19]	TFC-PAI	HF	0.66	0.32	0.48
I [36]	TFC-CNT	HF	2.45	0.12	0.05
J [38]	TFC-PES	HF	2.3	0.6	0.26
K [38]	TFC-PES	HF	2.3	0.5	0.22
L [35]	TFC-PEI	FS	2.31	0.29	0.13
M [39]	TFC-PEI	HF	2	0.1	0.05
N [28]	TFC-PES	HF	3.5	0.3	0.09
O [40]	TFC-PES	HF	3.5	0.3	0.09
P [41]	TFC-GO	FS	1.66	0.24	0.14
Q [42]	TFC-PVDF	FS	1.28	0.25	0.2
R [34]	TFC-PA	FS	1.63	1.42	0.87
S [34]	TFC-PA	FS	1.94	1.99	1.03
T [34]	TFC-PA	FS	1.5	3.76	2.51
U [43]	TFC-CAB	FS	2.85	0.35	0.12

There is a wide variety of membranes found in the literature made with different types of materials and module configurations. To simplify this analysis, the membranes will be classified in two groups: CTA-based membranes and TFC-based membranes. The reason to do this is because most of the commercial membranes are CTA-based and

in some cases they serve as a comparison to the newly developed membranes [27] [35] [36] [37] [38], whilst in the literature multiple TFC membranes are reported, all with improved characteristics that attempt to overcome the performance of commercial membranes under different conditions [20] [21] [35] [36] [37] [39] [40] [30] [41] [42] [43] [44]. In *Table 6* a selection of those membranes is shown. Five of the six CTA membranes were manufactured by Hydration Technologies, Inc. and the other one was manufactured by TOYOBO co. Even being manufactured by the same company, the five examples (A to E) have a wide range of values. This could be due to a diversity of reasons, such as changes in the manufacturing process, membrane storage previous to its usage, pre-treatment or the experimental conditions. These and other variables can affect directly the membrane performance and, therefore, the energy output. Moreover, it has been reported that CTA based membranes have "a poor chemical and biological stability", as explained in [21], which further suggest the usage of this kind of membranes should be avoided in real conditions.

Apart of the membrane composition, the module type plays an important role in the membrane overall performance. For example, flat sheets require spacers to allow the water flow through the membranes affecting their effectiveness [35] [12], while hollow fibers don't require them as their structures are self-supported [21]. In *Table 7* it can be seen that most of the membranes with a water permeability over 2 LMH/bar are of the HF type. From those FS with a relatively higher water permeability, L possess a nano-structure that improves the water flux and helps it to withstand higher pressures than other membranes [36]. Membrane U was developed with a different precursor than the usually studied esters and included post-treatment after the interfacial polymerization, aiming to enhance the properties [44]. In both cases, the results showed an improvement in the water permeability for FS membranes but not enough to surpass those provided by Loeb for a commercial membrane.

According to Loeb, in order to achieve a reasonable power output *A* value should be considerably high and *B* as low as possible. The original values for *A* and *B* in his article are 3.25 LMH/bar and 0.229 LMH, respectively [12]. The membrane used for those calculations was a TFC membrane for seawater desalination. Comparing those values with the ones shown on *Table 6*, most of the membranes have a lower performance overall. However, TFC-PES membranes G, N and O have a better water permeability

with a similar percentage ratio between this and their salt rejections (*B/A*), as can be seen in *Figure 7*.

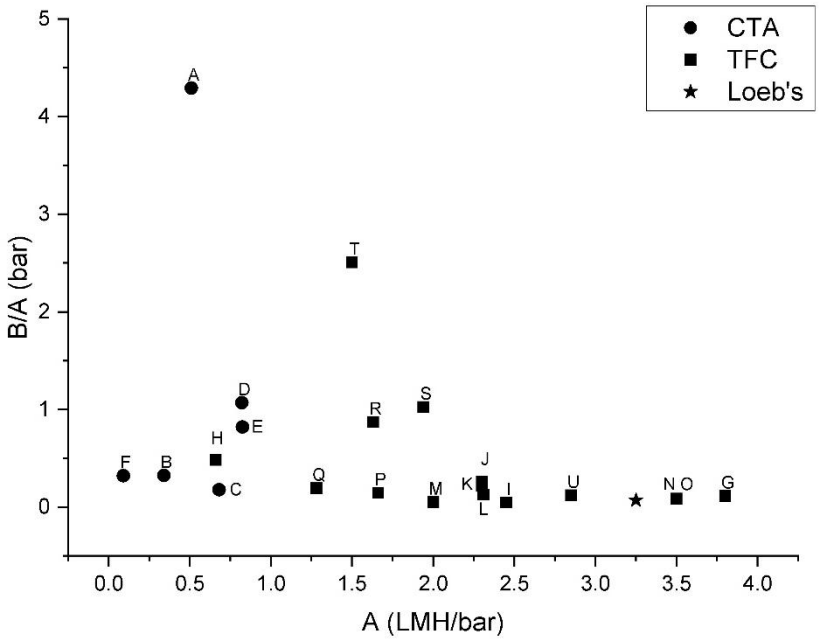

Figure 7. Variation of the parameter ratio B/A with water permeability for a wide range of forward osmosis membranes.

Even if the three sources of G, N and O analyse different properties of the membranes and PRO processes, they share similarities that could be considered for future developments. Membrane O source analyses a mathematical model for SWRO-PRO processes [41] using the properties from [50]. In [50] the authors developed a thin polyamide inner active layer by interfacial polymerization over a PES support hollow fiber. This method was followed to create membrane N with very similar results for *A* and *B* [30]. Membrane G was created with a similar method for interfacial polymerization that included $CaCl_2$ as a dopant for enhanced mechanical properties [20]. The membrane reported in [50] and membrane G share the same morphology of sponge-like structures beneath the active layer followed by finger-like structure at the support layer [20] [50]. It is acknowledged that the water content in the polymer dope during the polymerization process promotes the development of that morphology [20] [50]. Although this morphology may not the best for PRO processes [51], the membranes seem to withstand pressures over 15 bar [20] [50]. Knowing the factors that enhance the membrane performance allows us to develop methodologies for PRO-suitable designed membranes.

4.3. Water Flux Calculations

4.3.1. J_w under Field's membrane properties

The first group of values tested for J_w were those provided in [27]. They were divided in two sets, one obtained with a FS of 0 M and another of 0.025 M. The first one had an *A* value of 0.82 LMH*bar and the second of 0.67 LMH*bar. In both cases they had the same *B* of 0.88 LMH. Under those conditions it was possible to test *Equation (6)* and subsequently analyse the effects of salinity and mass transfer on it. Once they were tested with the base conditions as reported in [27], the k_c value was changed for those proposed in the methodology.

Figure 8 and *Figure 9* show the results obtained from those calculations. Figure 8 corresponds to the 0 M FS properties and *Figure 9* to the 0.025 M FS. As it can be observed both figures present a similar tendency but with better results when the properties for 0 M FS are used, as it is expected with a higher water permeability. While the results obtained for the Rivers-Seawater systems are very similar, [27] salinity conditions are outstanding in both figures. It can be acknowledge to the greater salinity difference existing in both cases (~57.84 g/kg), greater than the average in all the rivers (~35.25 g/kg).

It is clear in both figures that the results obtained with the highest value of k_c (50 µm/s) are the best overall. Comparing the results obtained for that k_c value and the original ones, [27] salinities show an improvement of 36-41% and the rivers of 25-30% (see *Figure 8* and *Figure 9*). The combination of a greater salinity difference and a high mass transfer coefficient at the active layer channel improves the water flux.

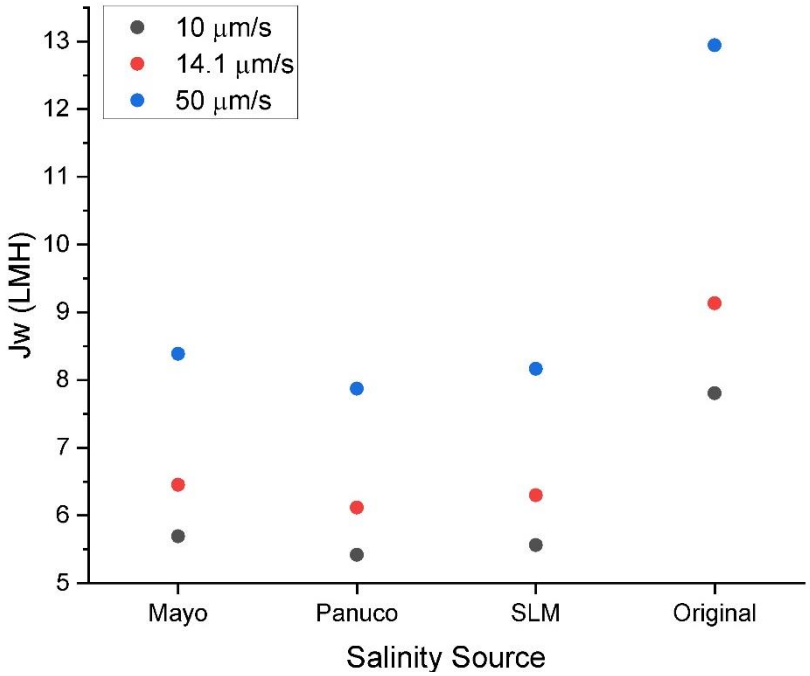

Figure 8. Water flux obtained using the parameters reported in [27] when FS is equal to 0 M. The river systems produce a lower water flux due their lower $\Delta\pi$.

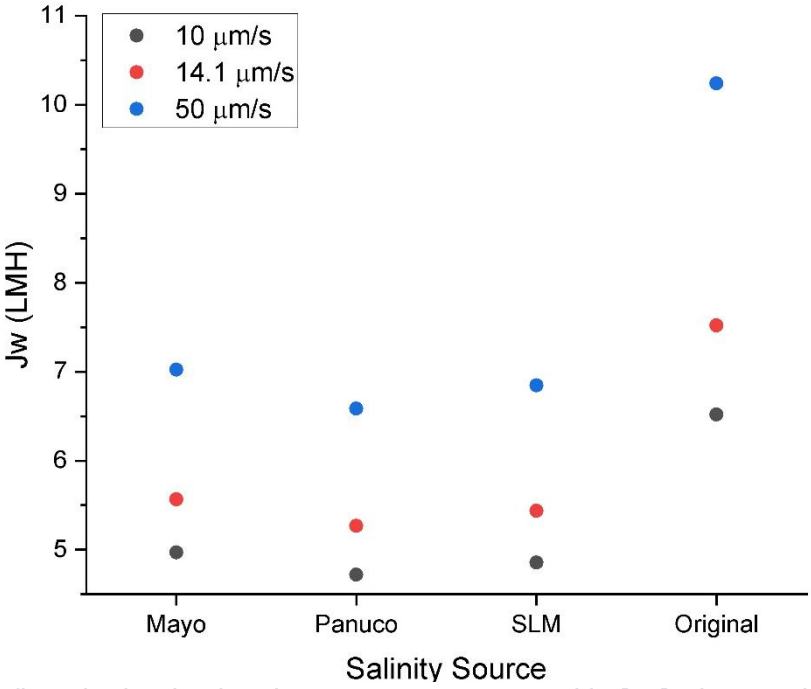

Figure 9. Water flux obtained using the parameters reported in [27] when FS is equal to 0.025 M. Compared to the results of the first set of values the water flux in this case decreases in all the scenarios.

4.3.2. J_w under Loeb's membrane properties

The article published by Loeb provides the values for water permeability (*A*) and salt rejection (*B*) of the employed membrane, which were used for this calculation. The membrane employed in Loeb' article possess a higher *A* and *B* (0.90 µm/s*bar and 0.64 µm/s respectively [12]) compared to those reported in [27], but like most of the actual membranes it wasn't developed specifically for PRO processes. Moreover, the values for mass transfer coefficient (*K* in his article) were assumptions rather the properties of the membrane itself [12]. Due to the lack of a *K* or k_c specific value for the membrane employed in [12] the calculations of this section will only consider the values of 10 µm/s and 50 µm/s for k_c, as 14.1 µm/s is an intrinsic property of the membrane analysed in [27].

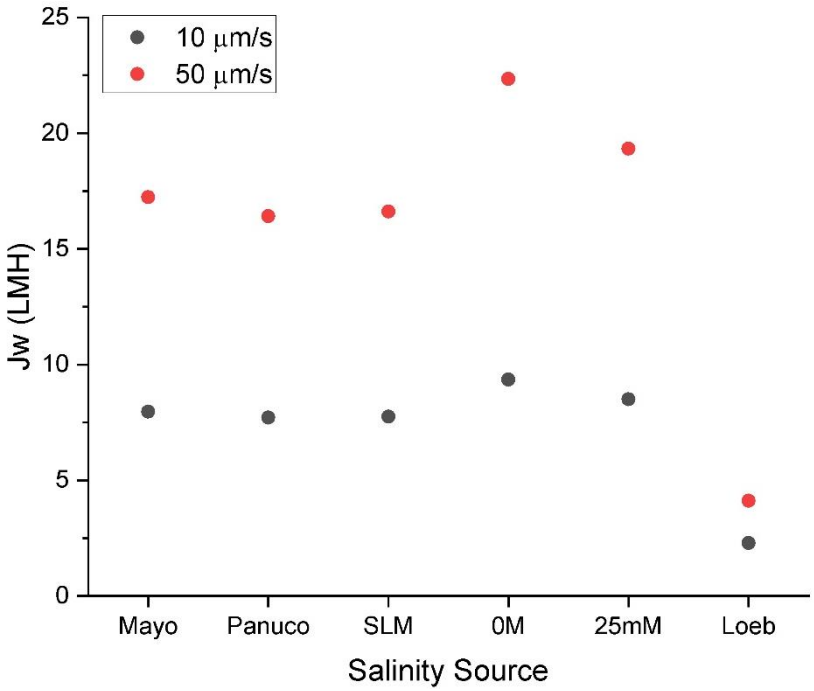

Figure 10. Water flux obtained using the parameters reported in [12]. Using [12] salinities the results are lower than with the rest of the scenarios.

Figure 10 presents the results under the mentioned conditions. Loeb's membrane have desirable properties (High *A* and low *B*) that allows the improvement of the J_w results

in all the scenarios but Loeb's due the salinity reported in his article. Rather than using the salinity values, the article reported two different pressures (π_{ds} and ΔP), and considering ΔP as the difference between the two water bodies osmotic pressures the third one (π_{fs}) can be calculated. ΔP is not as great as in the other salinity scenarios (12 bar vs. 12.56-22.57 bar) and it further decreases considering that only half of the ΔP is effective under the principle described in section 2.3 (see *Figure 3*). This can be observed in *Figure 10* where the results, even with a high k_c, are lower for Loeb's scenario. It can also be observed that, as mentioned in section 4.3.1., the greater salinity difference in combination with the mass transfer coefficient impact the water flux greatly.

4.3.3. J_w under membranes G, N and O properties

As in Loeb's case, k_c value is not provided by the original articles where G, N and O are found. Therefore, the same strategy was employed for the J_w calculation.

Figure 11 and *Figure 12* shows the water flux when k_c=10 µm/s and when k_c=50 µm/s. In both cases the same behaviour towards a greater salinity difference can be observed. Compared the results shown in *Figure 11* against those in *Figure 8* and *Figure 9*, and *Figure 12* against *Figure 10*, there is an existing improvement in the water flux. This is due the effect of a higher *A* and a relatively low *B* previously discussed in section 4.2.2.

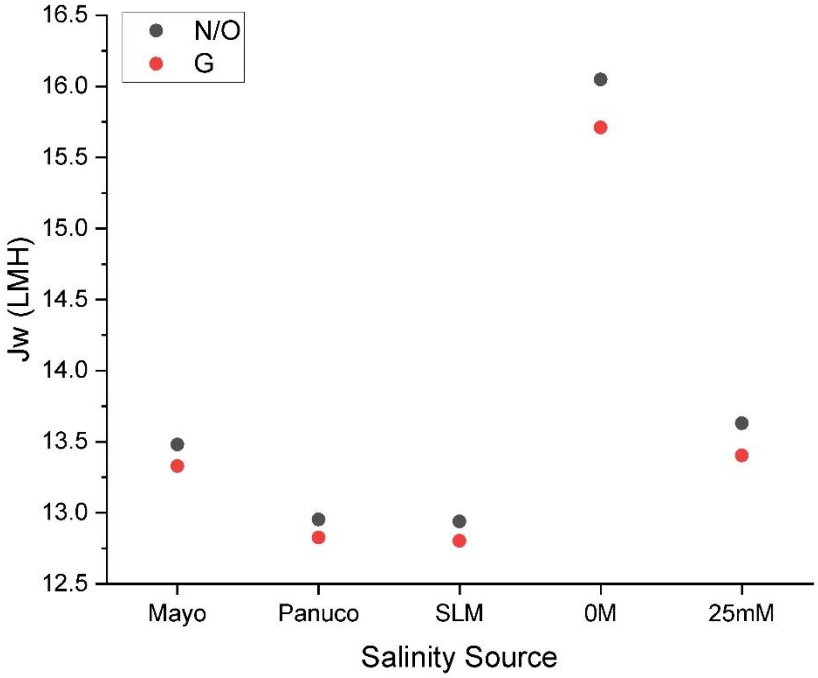

Figure 11. Water flux obtained using the parameters reported by different membranes with a low k_c value. The variation between G and N/O results is of ~0.12 µm/s in most of the cases.

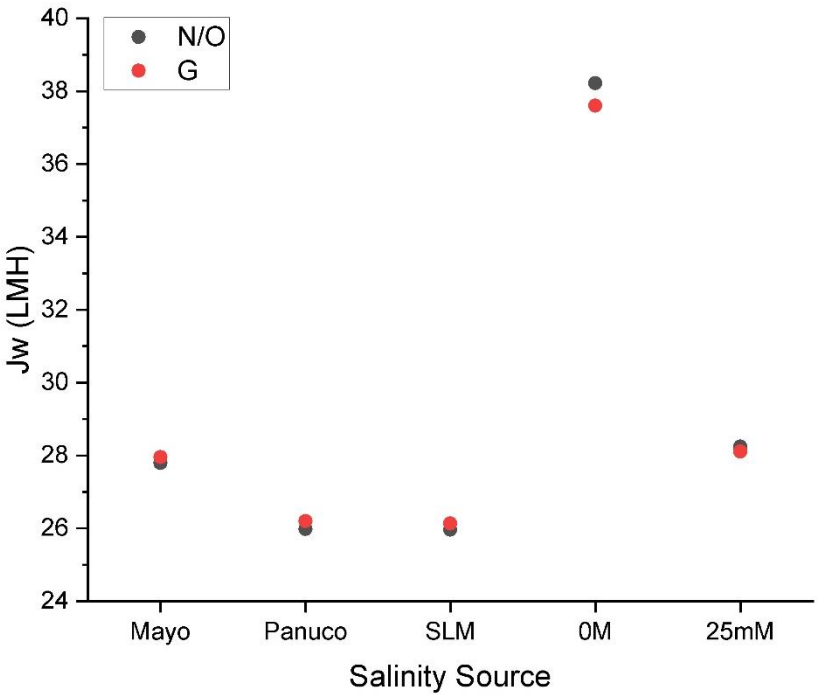

Figure 12.Water flux obtained using the parameters reported by different membranes with a high k_c value. All the results improved drastically considering those shown in Figure B.

Even with a noticeable increase in J_w, *Figure 12* doesn't present the same behaviour as *Figure 11* in all scenarios. The only two of them that follow the advantage of membrane N/O over G observed in *Figure 11* are those based on [27]. To understand the reasons behind this effect another set of calculations was run using all the salinities scenarios, fixing the values of A and B for those reported in membrane G and N/O and varying the values for k_c from 1 to 100. *Figure 13* Figure 14 show the results of those calculations.

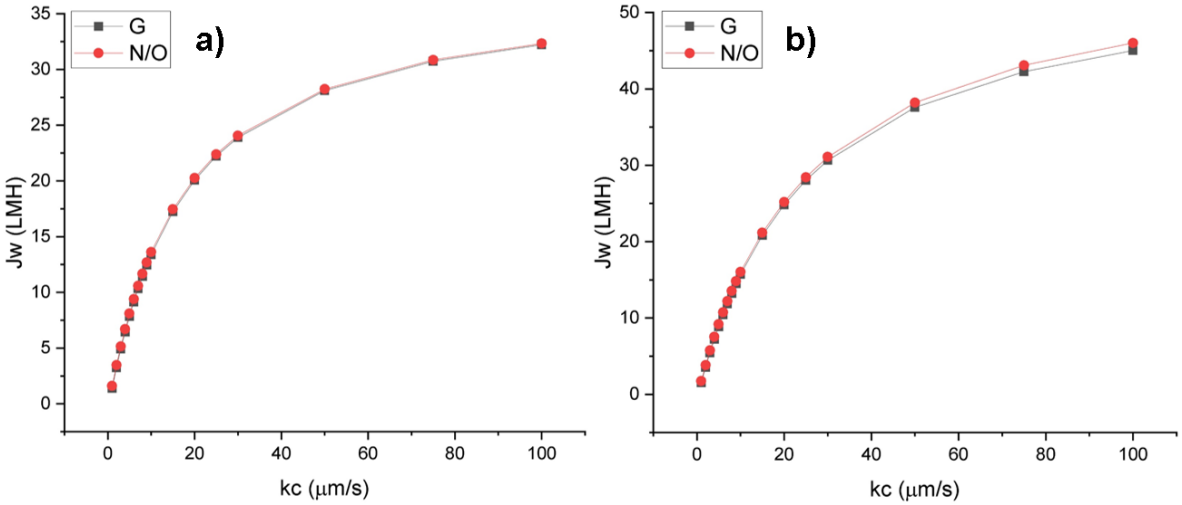

Figure 13 Analysis of the variability of J_w upon changes in k_c. a) correspond to the results when a 0 M solution is used as FS, and b) when 0.025 M is used as FS.

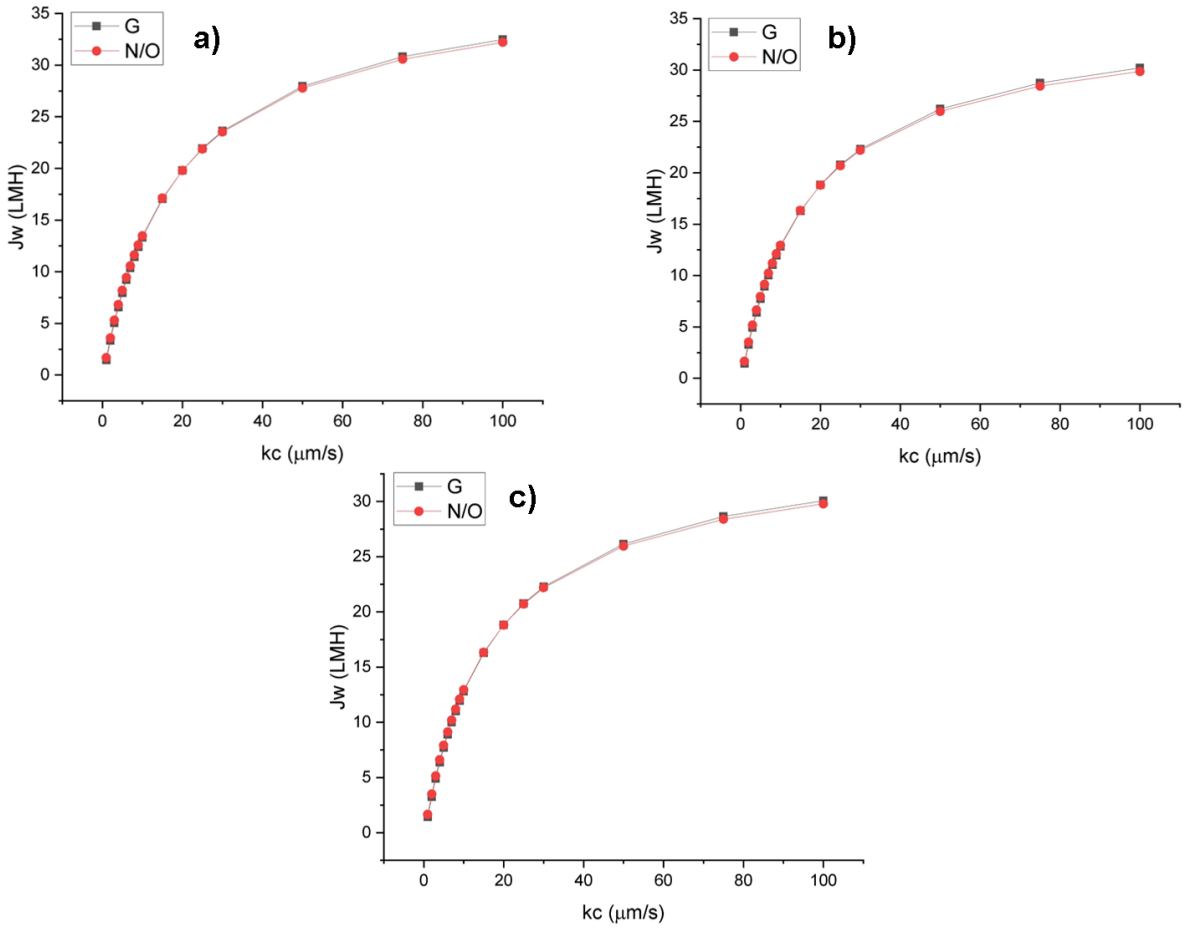

Figure 14. Analysis of the variability of J_w upon changes in kc using the Mayo (a), Panuco (b) and Soto La Marina (c) rivers salinities. In all three cases at the beginning of the curve membrane G shows a lower performance which later surpasses membrane N/O.

From *Figure 13* and *Figure 14* it can be asserted that there is an existing nonlinear correlation between k_c and J_w, and that the trend line will change depending of the water permeability (A), salt rejection (B), and salinity gradient. By using a logarithmic regression it is possible to obtain the equation of the curve for all the scenarios, then the intersection of the curves for G and N/O in each one of them (See *Table 7*). The results for [27] salinities follow the same tendency in all the analysed values of k_c having membrane G always with a performance below N/O, even if their intersection points are too low (0M) or too high (0.025M) in the X-axis (See *Table 7*). In the case of the rivers scenarios, their intersection points are located between the value of 10 and 50 µm/s. Once those values are surpassed the results give a small advantage to G over N/O, which can be observed in *Figure 13* and *Figure* 14, and it's fully consistent with the logarithmic nature of the equation itself. Although those calculations give us an overview of the possible behaviour of the membrane under the mentioned conditions,

the physical relation between the variables and the performance can only be analysed by testing the membranes in lab conditions.

Table 7. Equation of the curve and intersections in X (k_c) in each of the experiments shown in Figure 13 and Figure 14.

DS-Source	Membrane	Curve Equation (y)	R^2	Intersection (x)
0 M	G	10.539ln(x) - 6.0581	0.9579	0.445
	N/O	10.674ln(x) - 5.9487	0.957	
25 mM	G	7.5647ln(x) - 2.9107	0.9753	4078.116
	N/O	7.5296ln(x) - 2.6189	0.9759	
Mayo	G	7.5245ln(x) - 2.8358	0.9756	19.894
	N/O	7.3885ln(x) - 2.4291	0.9768	
Soto La Marina	G	6.9849ln(x) - 2.3094	0.9786	15.174
	N/O	6.833ln(x) - 1.8963	0.9798	
Panuco	G	6.9661ln(x) - 2.3032	0.9786	17.981
	N/O	6.8297ln(x) - 1.9091	0.9797	

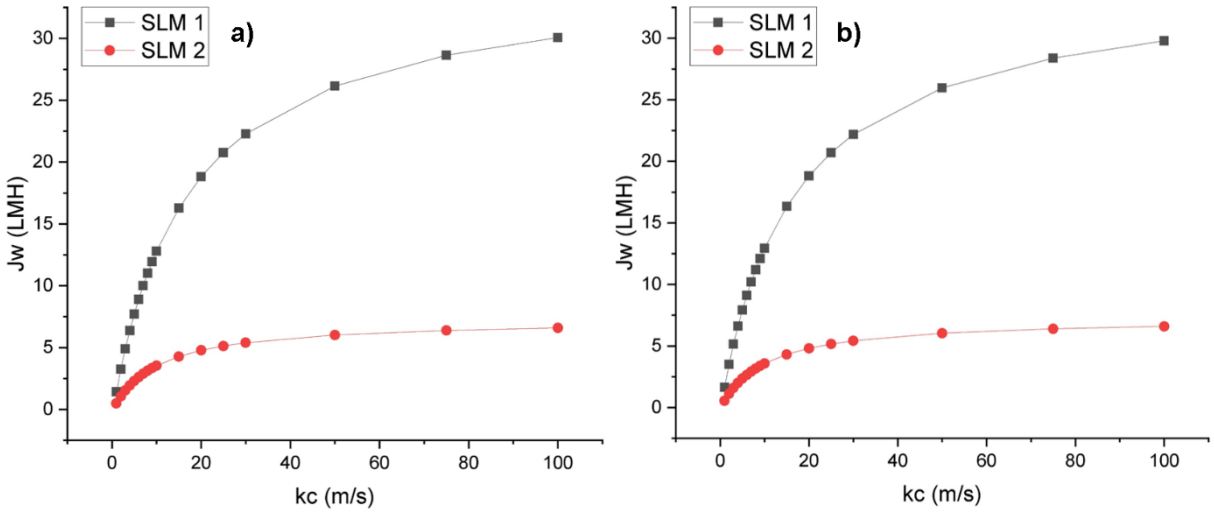

Figure 15. Comparison of the performance of membrane G (a) and N/O (b) using different DS-FS pairs. SLM 1 corresponds to the original salinity values from Soto La Marina River and SLM 2 to the proposed ones.

To understand the effect of salinity in this trend, another set of experiments was run with a fixed pressure difference (See *Figure 15*). In order to have a point of comparison, the ΔP of Soto La Marina River was chosen and π of DS and FS raised to 46 and 19.64 bar, respectively. The change in the osmotic pressure can only be done by changing the salinity of the solution, affecting its diffusivity. For the mentioned experiments, the water permeability and salt rejection remained the same.

The results of the original salinity values from Soto La Marina River promote a better water flux than the second set of values. This can be acknowledged to an increment in the salinity of the Feed Solution, which not only leads to a major loss of the theoretically possible water flux but, in real life, it can promote the fouling of that side of the membrane. It can be concluded that keeping the same salinity difference doesn't make an improvement in the water flux, thus increasing the salinity of both FS and DS decreases drastically J_w and furtherly affects the expected area power output.

4.4. W or Area Power

Figures *Figure* 16, *Figure* 17, *Figure* 18, *Figure* 19 and *Figure* 20 show the theoretical power generated with the previously calculated water fluxes. *Figure 16* and *Figure 17* correspond to the scenarios where values of *A* and *B* in [12] were employed for the calculation, *Figure 18* to Loeb's and *Figure 19* and *Figure 20* to G, N and O membranes.

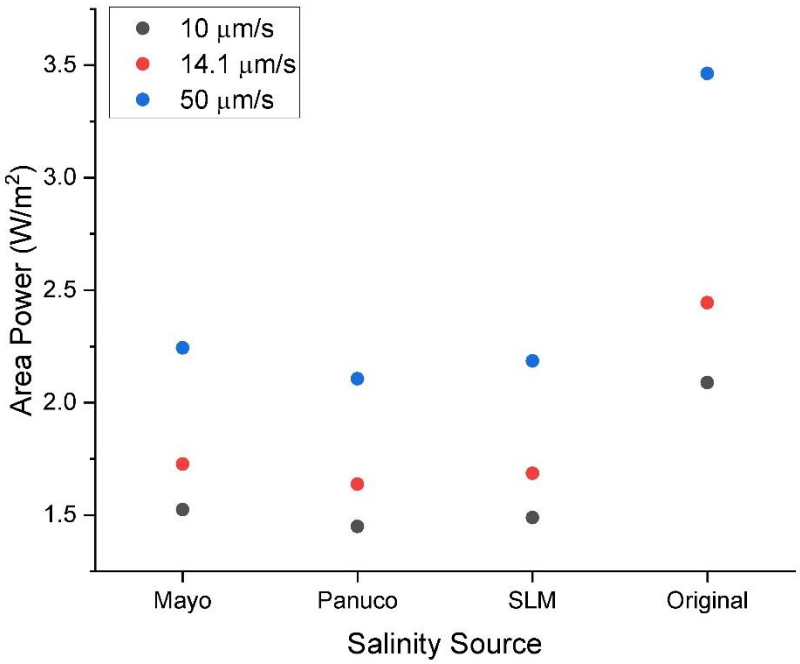

Figure 16.Area Power obtained under the parameters used for [27]. From the two properties reported in [27], those used in this case produce the highest power.

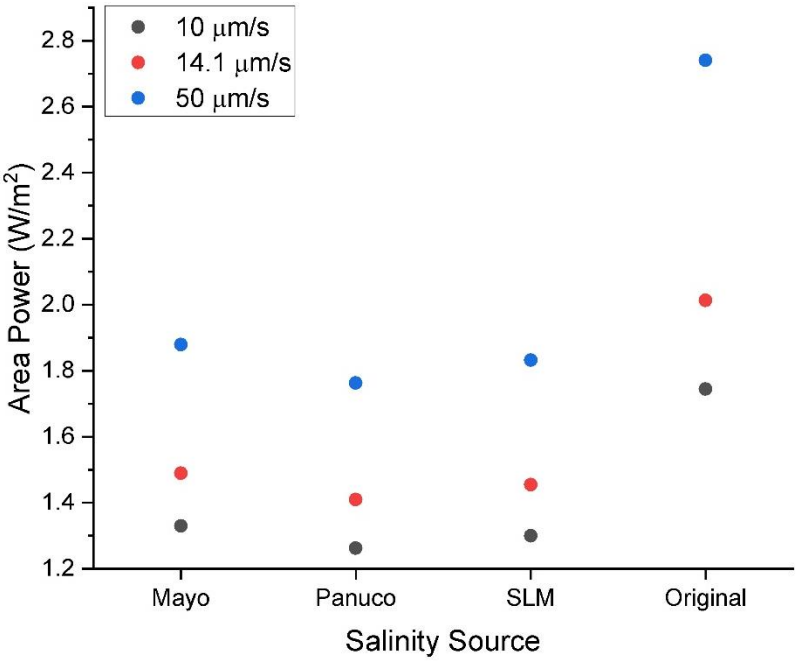

Figure 17. Area Power obtained under the parameters used for [27]. In this case, the water permeability was low enough to decrease ~0.4 W/m2.

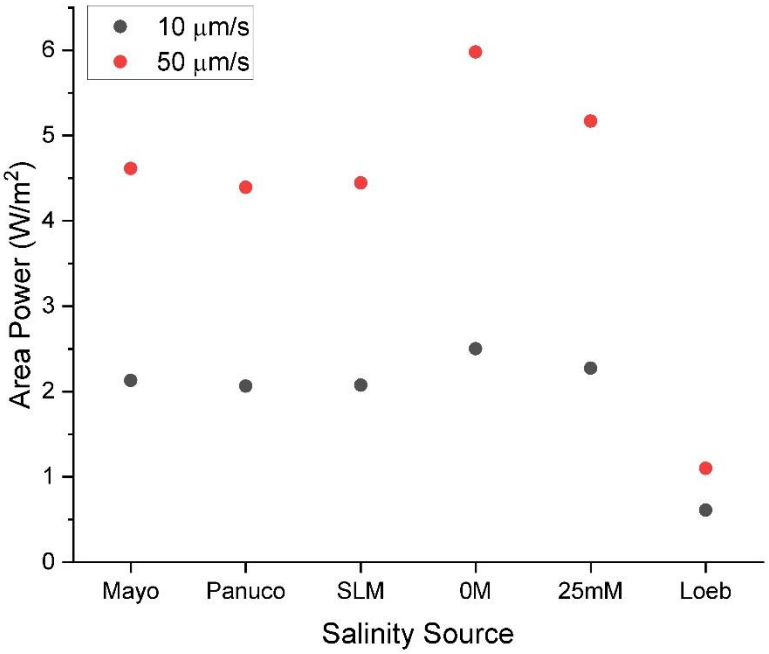

Figure 18. Area Power obtained under the parameters used for [12]. While under Loeb's salinities the results remain low, the other salinity scenarios present better results that could actually reach the goal of 5 W/m2.

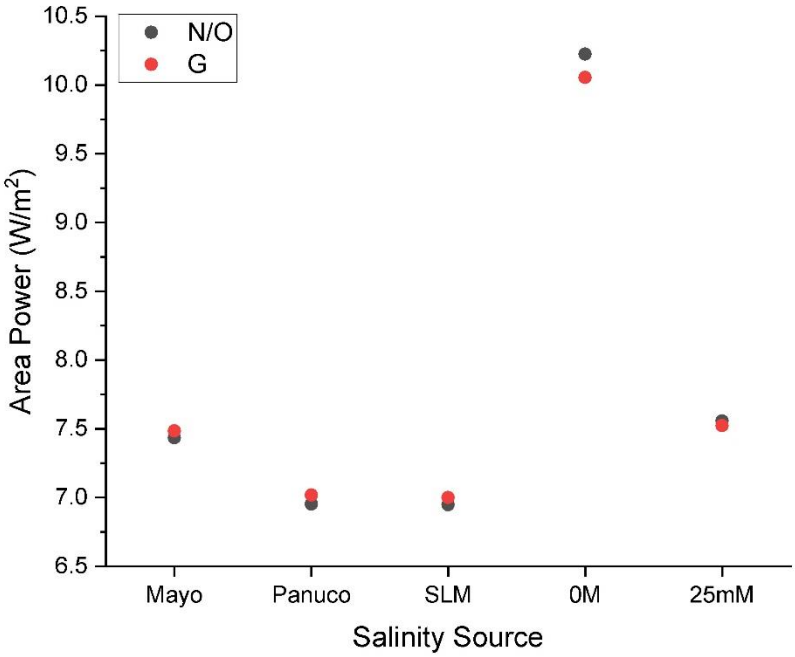

Figure 19. Area Power generated with the chosen membranes when kc=10 µm/s. Even with a low k_c value the results for all the scenarios are close to the goal. As in J_w analysis, membrane G presents a better performance than N/O.

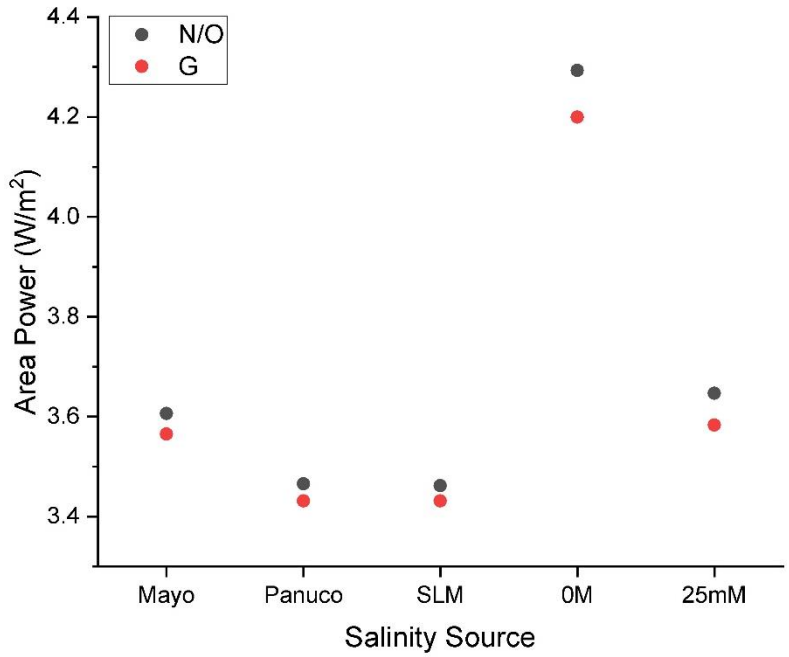

Figure 20. Area Power generated with the chosen membranes when kc=50 µm/s. Compared to Figure 16, in this figure are at least twice what could be obtained when kc=10 µm/s.

The tendency of the area power output seems not to vary regarding J_w, which could be interpreted that the same variables that affect J_w do affect *W* as well. This is consistent with the relation observed in equations *(6)* and *(7)* between all the variables mentioned before. From *Figure 16* and *Figure 17* it is clear that when the *A* value is higher the power output improves and that the proposed river-seawater systems will generate a lower output than those with a controlled salinity. However, even with the improved results none of the scenarios was able to reach 5 W/m^2 under the given conditions. From the previous observations it could be stated that the two options to increase the area power are to a) increase the salinity difference and, therefore, *ΔP*, b) enhancing the membrane properties (Especially *A* and *B*). It is also clear that from the three estuarine systems the Mayo River seems to have the highest possibilities of usage.

With the results obtained under Loeb's *A* and *B* (*Figure 18*) it can be argued that the previously reported results from [12] are not realistic anymore. Loeb's results are far beyond the rest of the scenarios due the salinity difference, even with a high k_c. However, the water permeability and salt rejection of the membranes reported by Loeb are better than those reported by [27], increasing the area power drastically. Comparing the results for Mayo River in *figures 13* and *15* there is an increment of 23.35% when k_c=10 µm/s and of 105.60% for k_c=50 µm/s. In the case of Panuco River, the increments are of 25.98% and 108.59% respectively. And for Soto La Marina River 23.11% and 103.42%. Loeb's membrane produces better results when k_c=50 µm/s generating power over the minimal stipulated in all the cases but its own salinities.

The behaviour previously discussed in section 4.3.3. can be observed in *Figure 19* and *Figure* 20 as well. Membrane N/O possess a better area power output while k_c is low and then changes this trend on the river scenarios once k_c increases. This is a confirmation of the effects that the DS-FS pair play in the overall performance. There is a substantial increment of the power output generated compared to those obtained with [27] reported membrane properties. With a k_c of 50 µm/s membrane G and N/O can reach a minimum of 6.9 W/m2 and a maximum of 10.2 W/m^2, which surpasses the proposed minimal area power output to make it sustainable. However, when k_c is low (*Figure 19*) the power is almost halved in all cases and doesn't reach the 5 W/m^2 goal. The highest area power generated by the rivers under this conditions is still ~70% the total that could be generated under [27] salinities.

Chapter 5. Conclusions and Future Work

5.1. Conclusions

This project has attempted to analyse the feasibility of PRO implementation in Mexico using real river-seawater scenarios and an improved formula to calculate the water flux for PRO under different scenarios, and to compare the results against a minimal area power output.

The analysed river-seawater scenarios present a high potential for PRO. From the three of them, Mayo River seems to have the highest possibility for a proper PRO plant development, but it is important to mention that all can reach easily the minimal required [13] with the usage of the right kind of membranes. One of the main obstacles for the actual implementation of PRO in those places is the collection of fresh water with a salinity low enough to harvest enough energy. For example, a ~50 km long pipe is not cost effective to consider it feasible, moreover it can cause an environmental impact that should be studied before its implementation. However, the usage of combined systems for desalination and PRO, like those employed in Mega-Ton project, could solve this issue promptly [11]. Therefore, with the right plant design and membrane technology there is a high potential for this technology in Mexico.

Most of the commercial membranes analysed in this project had a poor performance under PRO conditions, except for those with a TFC matrix. It can be considered that the TFC membranes have an enhanced performance compared to the CTA ones. Nevertheless, when developing new membranes it is important to focus not only in the material and easy production, but in the morphology and structure. It is necessary to find a balance between the ability to withstand high pressures and decreasing the salt flux and incrustations at the inner structure of the membranes. A higher water flux will help to increase the power output only when the solute permeability coefficient is low enough to not affect at all the process.

As stated before, in order to accurately calculate the feasibility of PRO plants nowadays it is important to consider the latest knowledge in mass transfer at ODMPs. The formula used to calculate the water flux in this document gives a more realistic overview of the performance accounting concentration polarization effects in the whole process. The results for J_w calculation demonstrates that there is an existing relation between the

performance and the membrane properties, consequently affecting the possible area power output of the system. Increasing the salinity difference could improve further the results but it will also imply that the risk of internal and external concentration polarization to happen will rise and other kind of strategies during the plant operation should be required. It is acknowledge that the plant design used for the area power calculation is based in an old RO plant and it should be updated to a newer one. However, Loeb's calculation design is flexible enough to adapt to any kind of plant and still been able to calculate the power properly.

In conclusion, PRO systems are a promising technology for the generation of energy. Their implementation could become a progress for green and sustainable energy. From this work, it can be stated that Mexico has a high potential for this kind of technology and it should be taken in account for the energy policies and projects developed in the country. Especially for the North of Mexico, PRO presents a possibility to deal with two of the biggest problems for the population: The water scarcity and the energy consumption. Therefore, the research of this kind of projects could make a change in the energy market not only in Mexico but all around the World.

5.2. Future Work

This project was mainly aimed to develop a way to calculate the possible energy production of PRO systems in real river-seawater situations in the North of Mexico. It is required to further research the kind of plant arrangement more suitable for the PRO process considering availability of low salinity water (DS) and the available membranes. Once it is done, calculate the energy production cost using formulas like those proposed by Loeb [12] will give a general overview of the plant feasibility. With this information it would be possible to propose this kind of projects for private or governmental investment.

As stated before, it is necessary to develop new membranes with enhanced properties fulfilling the requirements for PRO systems. This kind of membranes should have a structure able to withstand high pressures and stop salt intrusion to the inner layers of the membrane. Those membranes should not only be developed thinking in those properties, but also consider that their manufacturing process should be low cost to

make the PRO system feasible. It is also necessary to analyse which kind of module is the most suitable for this processes.

Lastly, the environmental impact of this kind of processes has not been assessed before as a whole. It is required to analyse it in order to create policies and regulations that allow to employ properly PRO as the sustainable green energy production process it could be.

Appendix 1. Data source

The following tables include the information provided by CNA for Mayo, Panuco and Soto La Marina River. The information was requested using the National Transparency Platform (https://www.plataformadetransparencia.org.mx/web/guest/inicio) on May 2nd, 2018, under the Request No. 1610100202618. The information included data regarding the location of the sampling points, dates, salinity, conductivity, dissolved solids and metals in the water matrixes. Only the information of location, dates and salinities is presented in the following tables. The names of each sampling point were given by the dependency but coded by the author of this document to simplify the analysis of the information. Due to the nature of the salinity analysis, there are four different values for salinity and an average. Depending of the deepness of the sampling sites, samples from the bottom, middle and superficial section of the water body would be collected and then analysed following standard procedures. In some cases, the results are below the Detection Limit (<DL) of the analysis and those values were considering as 0 for technical purposes. The cases where there is no data regarding salinity could be acknowledge to a change in the sampling objectives at those points (i.e. The value is no longer required) or the classification of the sampling point (i.e. High salinity water bodies are not considered for salinity analysis due the inaccuracy of the procedure to estimate a real value under those conditions). The analysis is done by an accredited laboratory hired by CNA, therefore, the sampling procedures could differ slightly in their detection limits and lead to different results but will always follow the same standards.

Table 8. Data from the Mayo River provided by CNA

Code	Date	Coordinates		Salinity (g/kg)				Average
		Latitude	Longitude	Initial	Bottom	Middle	Superficial	
M1	27/02/2015	26.73019	-109.7918	36	-	-	36	36.00
	12/04/2015	26.73019	-109.7918	37.6	-	-	37.6	37.60
	27/05/2015	26.73019	-109.7918	37.5	-	-	37.5	37.50
	21/07/2015	26.73019	-109.7918	36.9	38.1	36.8	36.9	37.27
	09/09/2015	26.73019	-109.7918	36.04	36.3	36.1	36.04	36.15
	20/10/2015	26.73019	-109.7918	33.8	33.8	33.8	33.8	33.80
	18/02/2016	26.73019	-109.7918	35	35.4	35	35	35.13
	14/04/2016	26.73019	-109.7918	32.8	-	-	36	36.00
	02/06/2016	26.73019	-109.7918	39.4	-	-	39.4	39.40
	20/07/2016	26.73019	-109.7918	40.4	-	-	39.6	39.60
	11/09/2016	26.73019	-109.7918	38	-	-	38	38.00

	05/10/2016	26.73019	-109.7918	38.6	-	-	38.6	38.60
	08/02/2017	26.73019	-109.7918	32.8	-	-	32.8	32.80
	26/03/2017	26.73019	-109.7918	34.1	-	-	34.1	34.10
	12/05/2017	26.73019	-109.7918	36.7	-	36.5	36.7	36.60
	11/07/2017	26.73019	-109.7918	35.2	-	35.3	35.2	35.25
	16/08/2017	26.73019	-109.7918	35.1	35.1	35.1	35.1	35.10
	08/10/2017	26.73019	-109.7918	35.50	-	35.5	35.50	35.50
M2	23/03/2015	27.0742	-109.50228	0.80	-	-	-	0.80
	12/05/2015	27.0742	-109.50228	0.02	-	-	-	0.02
	21/06/2015	27.0742	-109.50228	0.59	-	-	-	0.59
	30/07/2015	27.0742	-109.50228	0.61	-	-	-	0.61
	09/09/2015	27.0742	-109.50228	0.59	-	-	-	0.59
	07/10/2015	27.0742	-109.50228	0.15	-	-	-	0.15
	17/03/2016	27.0742	-109.50228	0.54	-	-	-	0.54
	04/05/2016	27.0742	-109.50228	0.59	-	-	-	0.59
	29/06/2016	27.0742	-109.50228	0.50	-	-	-	0.50
	27/09/2016	27.0742	-109.50228	0.27	-	-	-	0.27
	28/10/2016	27.0742	-109.50228	0.52	-	-	-	0.52
	11/11/2016	27.0742	-109.50228	0.50	-	-	-	0.50
	10/03/2017	27.0742	-109.50228	-	-	-	-	0.00
	28/04/2017	27.0742	-109.50228	-	-	-	-	0.00
	09/06/2017	27.0742	-109.50228	-	-	-	-	0.00
	28/07/2017	27.0742	-109.50228	-	-	-	-	0.00
	05/09/2017	27.0742	-109.50228	-	-	-	-	0.00
	22/10/2017	27.0742	-109.50228	-	-	-	-	0.00
M3	23/03/2015	27.11032	-109.42693	0.28	-	-	-	0.28
	12/05/2015	27.11032	-109.42693	0.02	-	-	-	0.02
	21/06/2015	27.11032	-109.42693	0.28	-	-	-	0.28
	29/07/2015	27.11032	-109.42693	0.32	-	-	-	0.32
	08/09/2015	27.11032	-109.42693	0.28	-	-	-	0.28
	07/10/2015	27.11032	-109.42693	0.14	-	-	-	0.14
	15/03/2016	27.11032	-109.42693	0.25	-	-	-	0.25
	04/05/2016	27.11032	-109.42693	0.27	-	-	-	0.27
	04/07/2016	27.11032	-109.42693	0.35	-	-	-	0.35
	02/09/2016	27.11032	-109.42693	0.16	-	-	-	0.16
	28/09/2016	27.11032	-109.42693	0.18	-	-	-	0.18
	12/12/2016	27.11032	-109.42693	0.20	-	-	-	0.20
	21/02/2017	27.11032	-109.42693	-	-	-	-	0.00
	18/04/2017	27.11032	-109.42693	-	-	-	-	0.00
	26/05/2017	27.11032	-109.42693	-	-	-	-	0.00
	12/07/2017	27.11032	-109.42693	-	-	-	-	0.00
	24/08/2017	27.11032	-109.42693	-	-	-	-	0.00
	22/10/2017	27.11032	-109.42693	-	-	-	-	0.00
M4	19/03/2015	27.1705	-109.366	0.21	-	-	-	0.21

	06/05/2015	27.1705	-109.366	0.01	-	-	-	0.01
	17/06/2015	27.1705	-109.366	0.18	-	-	-	0.18
	30/07/2015	27.1705	-109.366	0.13	-	-	-	0.13
	08/09/2015	27.1705	-109.366	0.11	-	-	-	0.11
	04/05/2016	27.1705	-109.366	0.21	-	-	-	0.21
	04/07/2016	27.1705	-109.366	0.21	-	-	-	0.21
	22/08/2016	27.1705	-109.366	0.23	-	-	-	0.23
	27/09/2016	27.1705	-109.366	0.21	-	-	-	0.21
	27/10/2016	27.1705	-109.366	0.20	-	-	-	0.20
	21/02/2017	27.1705	-109.366	-	-	-	-	0.00
	18/04/2017	27.1705	-109.366	-	-	-	-	0.00
	26/05/2017	27.1705	-109.366	-	-	-	-	0.00
	13/07/2017	27.1705	-109.366	-	-	-	-	0.00
	24/08/2017	27.1705	-109.366	-	-	-	-	0.00
	22/10/2017	27.1705	-109.366	-	-	-	-	0.00
M5	19/03/2015	27.2041	-109.189	0.12	-	-	-	0.12
	06/05/2015	27.2041	-109.189	0.01	-	-	-	0.01
	30/07/2015	27.2041	-109.189	0.16	-	-	-	0.16
	09/09/2015	27.2041	-109.189	0.14	-	-	-	0.14
	06/10/2015	27.2041	-109.189	0.15	-	-	-	0.15
	15/03/2016	27.2041	-109.189	0.14	-	-	-	0.14
	04/05/2016	27.2041	-109.189	0.14	-	-	-	0.14
	03/07/2016	27.2041	-109.189	0.17	-	-	-	0.17
	22/08/2016	27.2041	-109.189	0.17	-	-	-	0.17
	27/09/2016	27.2041	-109.189	0.10	-	-	-	0.10
	27/10/2016	27.2041	-109.189	0.14	-	-	-	0.14
	21/02/2017	27.2041	-109.189	-	-	-	-	0.00
	05/04/2017	27.2041	-109.189	-	-	-	-	0.00
	26/05/2017	27.2041	-109.189	-	-	-	-	0.00
	13/07/2017	27.2041	-109.189	-	-	-	-	0.00
	24/08/2017	27.2041	-109.189	-	-	-	-	0.00
	27/10/2017	27.2041	-109.189	-	-	-	-	0.00
M6	25/03/2015	27.2218	-109.00816	0.18	-	-	-	0.18
	12/05/2015	27.2218	-109.00816	0.05	-	-	-	0.05
	19/06/2015	27.2218	-109.00816	0.14	-	-	-	0.14
	31/07/2015	27.2218	-109.00816	0.09	-	-	-	0.09
	13/09/2015	27.2218	-109.00816	0.07	-	-	-	0.07
	06/10/2015	27.2218	-109.00816	0.13	-	-	-	0.13
	13/04/2016	27.2218	-109.00816	0.27	-	-	-	0.27
	02/09/2016	27.2218	-109.00816	0.12	-	-	-	0.12
	11/10/2016	27.2218	-109.00816	0.12	-	-	-	0.12
	03/11/2016	27.2218	-109.00816	0.10	-	-	-	0.10
	09/02/2017	27.2218	-109.00816	-	-	-	-	0.00
	17/08/2017	27.2218	-109.00816	-	-	-	-	0.00

	26/10/2017	27.2218	-109.00816	-	-	-	-	0.00
M7	23/03/2015	27.351	-108.92372	0.16	-	-	-	0.16
	07/05/2015	27.351	-108.92372	0.12	-	-	-	0.12
	17/06/2015	27.351	-108.92372	0.20	-	-	-	0.20
	02/08/2015	27.351	-108.92372	0.08	-	-	-	0.08
	10/09/2015	27.351	-108.92372	0.07	-	-	-	0.07
	05/10/2015	27.351	-108.92372	0.15	-	-	-	0.15
	16/03/2016	27.351	-108.92372	0.25	-	-	-	0.25
	03/05/2016	27.351	-108.92372	0.26	-	-	-	0.26
	28/06/2016	27.351	-108.92372	0.24	-	-	-	0.24
	01/09/2016	27.351	-108.92372	0.10	-	-	-	0.10
	28/09/2016	27.351	-108.92372	0.13	-	-	-	0.13
	28/10/2016	27.351	-108.92372	0.16	-	-	-	0.16
	26/02/2017	27.351	-108.92372	-	-	-	-	0.00
	17/04/2017	27.351	-108.92372	-	-	-	-	0.00
	02/06/2017	27.351	-108.92372	-	-	-	-	0.00
	12/07/2017	27.351	-108.92372	-	-	-	-	0.00
	23/08/2017	27.351	-108.92372	-	-	-	-	0.00
	24/10/2017	27.351	-108.92372	-	-	-	-	0.00
M8	23/03/2015	27.37488	-108.90729	0.16	-	-	-	0.16
	07/05/2015	27.37488	-108.90729	0.14	-	-	-	0.14
	17/06/2015	27.37488	-108.90729	0.22	-	-	-	0.22
	02/08/2015	27.37488	-108.90729	0.08	-	-	-	0.08
	10/09/2015	27.37488	-108.90729	0.07	-	-	-	0.07
	05/10/2015	27.37488	-108.90729	0.15	-	-	-	0.15
	16/03/2016	27.37488	-108.90729	0.23	-	-	-	0.23
	03/05/2016	27.37488	-108.90729	0.26	-	-	-	0.26
	28/06/2016	27.37488	-108.90729	0.25	-	-	-	0.25
	01/09/2016	27.37488	-108.90729	0.10	-	-	-	0.10
	28/09/2016	27.37488	-108.90729	0.12	-	-	-	0.12
	28/10/2016	27.37488	-108.90729	0.16	-	-	-	0.16
	26/02/2017	27.37488	-108.90729	-	-	-	-	0.00
	17/04/2017	27.37488	-108.90729	-	-	-	-	0.00
	02/06/2017	27.37488	-108.90729	-	-	-	-	0.00
	12/07/2017	27.37488	-108.90729	-	-	-	-	0.00
	23/08/2017	27.37488	-108.90729	-	-	-	-	0.00
	24/10/2017	27.37488	-108.90729	-	-	-	-	0.00

Table 9. Data from the Panuco River provided by the CNA.

Code	Date	Coordinates		Salinity (g/kg)				Average
		Latitude	Longitude	Initial	Bottom	Middle	Superficial	
P1	09/03/2015	22.2728	-97.7351	25.22	34.32	34.25	25.22	31.26
	02/05/2015	22.27289	-97.73391	22.06	33.98	33.74	22.06	29.93
	12/06/2015	22.27386	-97.73421	26.13	42.95	41.53	26.13	36.87
	24/07/2015	22.27181	-97.73362	18.89	37.11	37.52	18.89	31.17
	16/03/2016	22.27321	-97.73486	21	34	32.8	21	29.27
	04/05/2016	22.2729	-97.7354	32.63	32.3	32.6	32.63	32.51
	17/06/2016	22.2732	-97.735	36.93	37.7	37.6	36.93	37.41
	25/07/2016	22.2732	-97.7348	27.7	35.9	35.9	27.7	33.17
	04/04/2017	22.2733	-97.735	-	34.4	34.44	34.17	34.34
	21/05/2017	22.2734	-97.7349	-	37.9	37.85	37.7	37.82
	03/07/2017	22.2735	-97.7348	-	36.4	36.29	35.82	36.17
	31/08/2017	22.2732	-97.7348	-	40.8	40.6	38.6	40.00
P2	18/02/2015	22.2639	-97.777	9.38	33.21	15.48	9.38	19.36
	08/04/2015	22.2637	-97.77784	4.25	33.71	29.41	4.25	22.46
	21/05/2015	22.2628	-97.7819	7.78	35.2	31.2	7.78	24.73
	01/07/2015	22.2628	-97.7819	1.81	-	-	1.81	1.81
	11/10/2015	22.26325	-97.7835	29.5	51.93	29.57	29.5	37.00
	11/11/2015	22.2632	-97.7829	4.72	35.9	21.03	4.72	20.55
	02/03/2016	22.26296	-97.78335	15.7	35.8	34.2	15.7	28.57
	20/04/2016	22.26291	-97.78343	15.71	35.2	19.8	15.71	23.57
	01/06/2016	22.26309	-97.78345	13.2	31.1	28.5	13.2	24.27
	13/07/2016	22.2631	-97.7836	4.47	29.3	29.2	4.47	20.99
	24/08/2016	22.2631	-97.7835	2.37	-	-	-	2.37
	08/11/2016	22.2635	-97.7836	8.55	9.8	9.2	8.55	9.18
	13/03/2017	22.2628	-97.7835	12.24	30.8	21.3	12.24	21.45
	26/04/2017	22.2627	-97.7835	19.6	35.1	33.3	19.6	29.33
	05/06/2017	22.2631	-97.7837	32.7	26.9	32.6	32.71	30.74
	06/07/2017	22.263	-97.7834	10.35	35.3	22.4	10.36	22.69
	08/09/2017	22.2631	-97.7836	2.74	-	-	-	2.74
	09/10/2017	22.2626	-97.7839	0.25	-	-	-	0.25
P3	18/02/2015	22.25396	-97.80605	9.11	37.38	27.23	9.11	24.57
	08/04/2015	22.2548	-97.8042	3.76	33.93	33.01	3.36	23.43
	21/05/2015	22.25353	-97.80716	6.02	35.71	30.13	6.02	23.95
	01/07/2015	22.25382	-97.80917	1.79	-	-	1.79	1.79
	11/10/2015	22.25435	-97.80739	11.35	58.06	11.15	11.35	26.85
	11/11/2015	22.2538	-97.8079	3.59	35.7	8.27	3.59	15.85
	02/03/2016	22.2541	-97.8064	13.32	33	31.1	13.32	25.81
	20/04/2016	22.2529	-97.8089	9.52	25.7	15.1	9.52	16.77
	01/06/2016	22.254	-97.8063	9.8	26.4	22	9.8	19.40
	13/07/2016	22.2535	-97.8064	5.86	28.4	25.8	5.86	20.02

	24/08/2016	22.2546	-97.8069	1.92	15.3	2.3	15.3	10.97
	08/11/2016	22.2544	-97.8068	8.93	9.2	9.1	8.93	9.08
	13/03/2017	22.254	-97.8071	11.72	31.7	32.7	11.72	25.37
	26/04/2017	22.2538	-97.8071	17.55	33.7	31.3	17.55	27.52
	05/06/2017	22.2541	-97.8066	15.12	32	32.6	15.12	26.57
	06/07/2017	22.2543	-97.8063	7.4	33.8	13.6	7.43	18.28
	08/09/2017	22.2543	-97.8067	1.77	-	-	-	1.77
	09/10/2017	22.2542	-97.8055	0.49	-	-	-	0.49
P4	18/02/2015	22.24544	-97.81991	7.01	31	24.7	7.01	20.89
	08/04/2015	22.2454	-97.8206	3.86	33	24.9	3.86	20.63
	21/05/2015	22.2449	-97.8204	5.81	35	28.0	5.81	23.03
	01/07/2015	22.245	-97.8226	1.75	-	-	1.75	1.75
	11/10/2015	22.2456	-97.8229	12.83	51	23.8	12.83	29.08
	12/11/2015	22.24533	-97.8228	3.10	18	4.7	3.10	8.76
	02/03/2016	22.2447	-97.8238	11.18	35	28.7	11.18	24.96
	20/04/2016	22.24558	-97.82256	7.75	26	16.0	7.75	16.45
	01/06/2016	22.245	-97.8229	9.50	25	20.5	9.50	18.23
	13/07/2016	22.2456	-97.8228	5.66	25	24.0	5.66	18.09
	24/08/2016	22.2455	-97.8227	1.35	15	1.9	15.06	10.69
	08/11/2016	22.2456	-97.8227	7.30	9	8.6	7.30	8.20
	13/03/2017	22.245	-97.8237	11.05	36	15.2	11.05	20.62
	26/04/2017	22.245	-97.8232	11.75	32	27.1	11.75	23.48
	05/06/2017	22.2456	-97.8228	11.20	33	31.4	11.20	25.20
	06/07/2017	22.245	-97.8228	8.85	34	9.4	8.85	17.32
	07/08/2017	22.2458	-97.8231	9.34	33	36.6	9.34	26.28
	09/10/2017	22.2447	-97.8222	0.78	-	-	-	0.78
P5	18/02/2015	22.22859	-97.8352	5.86	25.86	23.99	5.86	18.57
	08/04/2015	22.2279	-97.8344	1.7	33.02	32.88	1.7	22.53
	21/05/2015	22.22815	-97.83421	6.92	35.17	31.72	6.92	24.60
	01/07/2015	22.2285	-97.8368	1.76	-	-	1.76	1.76
	11/10/2015	22.2294	-97.8377	9.03	40.27	20.66	9.03	23.32
	12/11/2015	22.2295	-97.83781	3.06	15.59	4.82	3.06	7.82
	02/03/2016	22.22849	-97.83689	11.63	30.7	27.2	11.63	23.18
	20/04/2016	22.2293	-97.83786	7.92	29.2	18.3	7.92	18.47
	01/06/2016	22.23017	-97.83782	6.67	29.4	28.1	6.67	21.39
	13/07/2016	22.2301	-97.8378	2.91	22	18.4	18.38	19.59
	25/08/2016	22.2298	-97.8372	0.97	24.3	18.6	18.58	20.49
	22/11/2016	22.2299	-97.8384	2.65	-	-	-	2.65
	13/03/2017	22.2294	-97.8378	9.03	35.5	22.5	9.03	22.34
	26/04/2017	22.2297	-97.8379	10.32	29.9	25.4	10.32	21.87
	05/06/2017	22.2297	-97.8378	8.81	32	32.7	8.81	24.50
	06/07/2017	22.23	-97.8377	7.22	34.3	13.1	7.22	18.21
	07/08/2017	22.2301	-97.8376	6.06	23.7	12.2	6.06	13.99
	09/10/2017	22.2297	-97.8376	0.3	-	-	-	0.30

P6	06/02/2015	22.22282	-97.89576	1.5	-	-	1.5	1.50
	23/03/2015	22.22274	-97.89544	1.7	-	-	1.7	1.70
	01/05/2015	22.2224	-97.8953	1.39	-	-	1.39	1.39
	11/06/2015	22.223	-97.8952	< DL	-	-	<DL	< DL
	27/07/2015	22.2232	-97.8962	0.83	-	-	0.83	0.83
	21/10/2015	22.2228	-97.8953	2.31	-	-	2.31	2.31
	09/03/2016	22.2228	-97.8959	6.34	17.4	6.3	6.34	10.01
	12/04/2016	22.2228	-97.896	6.94	29.2	12.5	6.94	16.21
	17/05/2016	22.22282	-97.89619	9.07	30.4	9.1	9.07	16.19
	28/08/2016	22.2228	-97.8961	0.32	-	-	-	0.32
	02/10/2016	22.2228	-97.8961	0.27	-	-	-	0.27
	12/11/2016	22.2228	-97.8961	0.36	-	-	-	0.36
	13/03/2017	22.2226	-97.8965	4.05	33.8	22.7	4.05	20.18
	25/04/2017	22.2228	-97.896	4.09	-	11.9	4.09	8.00
	01/07/2017	22.2228	-97.8958	4.5	6.3	5.8	4.5	5.53
	04/08/2017	22.2229	-97.8959	2.53	-	-	-	2.53
	18/09/2017	22.2229	-97.8959	0.25	-	-	-	0.25
	19/10/2017	22.2229	-97.8961	0.29	-	-	-	0.29
P7	06/02/2015	22.18384	-98.01583	0.34	-	-	0.34	0.34
	23/03/2015	22.1842	-98.0157	< DL	-	-	< DL	0.00
	01/05/2015	22.1845	-98.0159	< DL	-	-	< DL	0.00
	11/06/2015	22.18385	-98.01578	< DL	-	-	< DL	0.00
	27/07/2015	22.18452	-98.01568	< DL	-	-	< DL	0.00
	21/10/2015	21.18449	-98.01561	0.78	-	-	0.78	0.78
	09/03/2016	22.18436	-98.0155	3.42	-	-	-	3.42
	12/04/2016	22.18387	-98.0154	4.67	-	-	-	4.67
	17/05/2016	22.1844	-98.0156	1.39	-	-	-	1.39
	28/08/2016	22.1843	-98.0154	0.31	-	-	-	0.31
	11/11/2016	22.1843	-98.0154	0.33	-	-	-	0.33
	29/11/2016	22.1841	-98.0157	0.3	-	-	-	0.30
	15/02/2017	22.1841	-98.0152	-	-	-	-	0.00
	11/04/2017	22.1838	-98.0157	-	-	-	-	0.00
	07/06/2017	22.1839	-98.0155	-	-	-	-	0.00
	23/07/2017	22.1855	-98.0157	-	-	-	-	0.00
	06/09/2017	22.1841	-98.0153	-	-	-	-	0.00
	11/10/2017	22.1848	-98.0152	-	-	-	-	0.00
P8	06/02/2015	22.1312	-98.0638	0.44	-	-	0.44	0.44
	23/03/2015	22.1313	-98.0642	< DL	-	-	< DL	0.00
	01/05/2015	22.13191	-98.06454	< DL	-	-	< DL	0.00
	11/06/2015	22.1308	-98.0608	< DL	-	-	< DL	0.00
	27/07/2015	22.13119	-98.0636	< DL	-	-	< DL	0.00
	21/10/2015	21.13188	-98.06328	0.7	-	-	0.7	0.70
	09/03/2016	22.1306	-98.0605	1.56	-	-	-	1.56
	12/04/2016	22.13051	-98.06008	1.83	-	-	-	1.83

	17/05/2016	22.131	-98.0609	0.79	-	-	-	0.79
	28/08/2016	22.1306	-98.0608	0.3	-	-	-	0.30
	09/10/2016	22.1306	-98.0609	0.3	-	-	-	0.30
	12/11/2016	22.1309	-98.0604	0.32	-	-	-	0.32
	15/02/2017	22.1305	-98.0607	-	-	-	-	0.00
	11/04/2017	22.1303	-98.0614	-	-	-	-	0.00
	07/06/2017	22.1303	-98.061	-	-	-	-	0.00
	23/07/2017	22.1308	-98.0605	-	-	-	-	0.00
	06/09/2017	22.1306	-98.0608	-	-	-	-	0.00
	11/10/2017	22.1308	-98.0608	-	-	-	-	0.00
P9	24/02/2015	22.05997	-98.1766	0	-	-	-	0.00
	16/04/2015	22.06	-98.1766	< DL	-	-	-	0.00
	03/06/2015	22.05993	-98.17667	< DL	-	-	-	0.00
	21/07/2015	22.06	-98.17657	< DL	-	-	-	0.00
	16/10/2015	22.05995	-98.17653	< DL	-	-	-	0.00
	16/11/2015	22.06	-98.1764	< DL	-	-	-	0.00
	01/03/2016	22.0598	-98.1769	0.55	-	-	-	0.55
	07/04/2016	22.05989	-98.17674	0.56	-	-	-	0.56
	11/05/2016	22.0599	-98.1768	0.57	-	-	-	0.57
	11/09/2016	22.0599	-98.1768	0.33	-	-	-	0.33
	09/10/2016	22.0599	-98.1768	0.29	-	-	-	0.29
	11/11/2016	22.0599	-98.1767	0.31	-	-	-	0.31
	22/02/2017	22.0598	-98.1768	-	-	-	-	0.00
	12/04/2017	22.0599	-98.1768	-	-	-	-	0.00
	06/06/2017	22.0594	-98.1763	-	-	-	-	0.00
	18/07/2017	22.0599	-98.1767	-	-	-	-	0.00
	14/09/2017	22.06	-98.1766	-	-	-	-	0.00
	16/10/2017	22.0597	-98.1771	-	-	-	-	0.00
P10	24/02/2015	22.09205	-98.19297	0	-	-	-	0.00
	16/04/2015	22.09201	-98.19294	< DL	-	-	-	0.00
	03/06/2015	22.0915	-98.19266	< DL	-	-	-	0.00
	21/07/2015	22.0917	-98.1932	< DL	-	-	-	0.00
	16/10/2015	22.092	-98.193	< DL	-	-	-	0.00
	16/11/2015	22.0919	-98.1935	< DL	-	-	-	0.00
	01/03/2016	22.0911	-98.1922	0.54	-	-	-	0.54
	07/04/2016	22.09111	-98.19219	0.57	-	-	-	0.57
	11/05/2016	22.0912	-98.1922	0.58	-	-	-	0.58
	11/09/2016	22.0915	-98.193	0.33	-	-	-	0.33
	09/10/2016	22.0915	-98.1932	0.3	-	-	-	0.30
	11/11/2016	22.0908	-98.1925	0.52	-	-	-	0.52
	15/02/2017	22.0917	-98.1927	-	-	-	-	0.00
	11/04/2017	22.0914	-98.1923	-	-	-	-	0.00
	06/06/2017	22.0908	-98.1934	-	-	-	-	0.00
	23/07/2017	22.0912	-98.1928	-	-	-	-	0.00

	06/09/2017	22.0919	-98.1932	-	-	-	-	0.00
	11/10/2017	22.0915	-98.1932	-	-	-	-	0.00

Table 10. Data from the Soto La Marina River provided by the CNA.

Code	Date	Coordinates		Salinity (g/kg)				Average
		Latitude	Longitude	Initial	Bottom	Middle	Superficial	
S1	24/02/2015	23.77457	-97.73228	33.87	-	-	33.87	33.87
	14/04/2015	23.7748	-97.732	33.54	-	-	33.54	33.54
	02/06/2015	23.7749	-97.7321	34.81	-	-	34.81	34.81
	22/07/2015	23.7748	-97.7322	39.5	-	-	39.5	39.50
	14/03/2016	23.77435	-97.73402	33.86	-	-	33.86	33.86
	02/05/2016	23.7743	-97.7342	35.8	-	-	35.8	35.80
	16/06/2016	23.7742	-97.7342	37.08	-	-	37.08	37.08
	26/07/2016	23.7743	-97.7342	36.88	-	-	36.88	36.88
	19/03/2017	23.7749	-97.7343	-	-	-	36.3	36.30
	25/04/2017	23.7744	-97.7344	-	-	-	36.93	36.93
	15/06/2017	23.774	-97.7344	-	-	-	34.3	34.30
	30/07/2017	23.7743	-97.7344	-	-	-	37.8	37.80
S2	24/02/2015	23.773	-97.7352	32.92	-	-	32.92	32.92
	14/04/2015	23.77268	-97.73558	33.22	34.25	-	33.22	33.74
	02/06/2015	23.773	-97.7354	34.38	34.57	-	34.38	34.48
	22/07/2015	23.77249	-97.73523	3.01	-	-	3.01	3.01
	14/03/2016	23.7731	-97.7381	34.51	33.4	34.3	34.51	34.07
	12/05/2016	23.7729	-97.7376	34.72	35.1	35	34.72	34.94
	16/06/2016	23.7728	-97.7376	27.18	-	28.4	27.18	27.79
	26/07/2016	23.7729	-97.7377	28.43	-	29.9	28.43	29.17
	19/03/2017	23.773	-97.7378	36.11	-	-	36.11	36.11
	25/04/2017	23.7731	-97.7377	35.33	35.4	-	35.33	35.37
	15/06/2017	23.7729	-97.7377	35.2	-	-	35.2	35.20
	16/07/2017	23.773	-97.7376	33.97	33.9	-	33.97	33.94
	23/08/2017	23.7728	-97.7375	38.89	38.9	38.9	38.89	38.90
	04/10/2017	23.7729	-97.7378	33.33	35.5	34.7	33.33	34.51
S3	25/02/2015	23.73763	-98.20435	< DL	-	-	-	0.00
	10/04/2015	23.73766	-98.20439	< DL	-	-	-	0.00
	20/05/2015	23.73787	-98.20443	< DL	-	-	-	0.00
	06/07/2015	23.7376	-98.2044	< DL	-	-	-	0.00
	14/08/2015	23.73765	-98.20435	0.57	-	-	-	0.57
	13/11/2015	23.7378	-98.2064	< DL	-	-	-	0.00
	14/06/2016	23.7376	-98.2066	0.71	-	-	-	0.71
	27/07/2016	23.7375	-98.2066	0.69	-	-	-	0.69
	08/09/2016	23.7376	-98.2066	0.77	-	-	-	0.77
	14/10/2016	23.7377	-98.2066	0.67	-	-	-	0.67
	16/03/2017	23.7376	-98.2067	-	-	-	-	-

	02/05/2017	23.7377	-98.2065	-	-	-	-	-
	27/06/2017	23.7372	-98.2061	-	-	-	-	-
	01/08/2017	23.7375	-98.2067	-	-	-	-	-
	05/09/2017	23.7376	-98.2067	-	-	-	-	-
	08/10/2017	23.7374	-98.2066	-	-	-	-	-
S4	25/02/2015	23.7912	-98.2018	< DL	-	-	-	0.00
	10/04/2015	23.7913	-98.20184	< DL	-	-	-	0.00
	20/05/2015	23.79126	-98.20178	< DL	-	-	-	0.00
	06/07/2015	23.79159	-98.20188	< DL	-	-	-	0.00
	14/08/2015	23.7912	-98.2018	< DL	-	-	-	0.00
	05/10/2015	23.79117	-98.20381	1.25	-	-	-	1.25
	14/06/2016	23.7912	-98.2039	0.7	-	-	-	0.70
	27/07/2016	23.7914	-98.204	0.59	-	-	-	0.59
	08/09/2016	23.7914	-98.204	0.94	-	-	-	0.94
	14/10/2016	23.792	-98.2042	0.68	-	-	-	0.68
	16/03/2017	23.7913	-98.2039	-	-	-	-	0.00
	02/05/2017	23.7914	-98.2039	-	-	-	-	0.00
	30/06/2017	23.7915	-98.2039	-	-	-	-	0.00
	01/08/2017	23.7912	-98.204	-	-	-	-	0.00
	01/11/2017	23.7916	-98.2041	-	-	-	-	0.00
S5	25/02/2015	23.83086	-98.20379	< DL	-	-	-	0.00
	10/04/2015	23.8309	-98.2038	< DL	-	-	-	0.00
	20/05/2015	23.8316	-98.2034	< DL	-	-	-	0.00
	06/07/2015	23.83201	-98.20274	< DL	-	-	-	0.00
	14/08/2015	23.83109	-98.20369	< DL	-	-	-	0.00
	05/10/2015	23.83228	-98.20532	1.24	-	-	-	1.24
	15/03/2016	23.8324	-98.2051	0.77	-	-	-	0.77
	03/05/2016	23.83237	-98.20494	0.53	-	-	-	0.53
	14/06/2016	23.8325	-98.205	0.92	-	-	-	0.92
	27/07/2016	23.8324	-98.205	0.6	-	-	-	0.60
	08/09/2016	23.8325	-98.205	0.86	-	-	-	0.86
	14/10/2016	23.8325	-98.2051	0.66	-	-	-	0.66
	16/03/2017	23.8324	-98.205	-	-	-	-	0.00
	02/05/2017	23.8324	-98.205	-	-	-	-	0.00
	30/06/2017	23.8319	-98.2049	-	-	-	-	0.00
	31/07/2017	23.8324	-98.205	-	-	-	-	0.00
	05/09/2017	23.8325	-98.205	-	-	-	-	0.00
	05/10/2017	23.8323	-98.2053	-	-	-	-	0.00
S6	25/02/2015	23.99852	-98.26859	< DL	-	-	-	0.00
	10/04/2015	23.9985	-98.2686	< DL	-	-	-	0.00
	20/05/2015	23.99853	-98.26865	< DL	-	-	-	0.00
	06/07/2015	23.9987	-98.26852	< DL	-	-	-	0.00
	14/08/2015	23.9985	-98.2686	< DL	-	-	-	0.00
	05/10/2015	23.99862	-98.27067	0.94	-	-	-	0.94

	15/03/2016	23.99845	-98.27046	0.64	-	-	-	0.64
	03/05/2016	23.99844	-98.27046	0.48	-	-	-	0.48
	14/06/2016	23.9984	-98.2704	0.58	-	-	-	0.58
	27/07/2016	23.9984	-98.2704	0.48	-	-	-	0.48
	08/09/2016	23.9985	-98.2704	0.63	-	-	-	0.63
	14/10/2016	23.9986	-98.2707	0.54	-	-	-	0.54
	16/03/2017	23.9984	-98.2705	-	-	-	-	0.00
	02/05/2017	23.9986	-98.2707	-	-	-	-	0.00
	30/06/2017	23.9982	-98.2704	-	-	-	-	0.00
	01/08/2017	23.9985	-98.2704	-	-	-	-	0.00
	05/09/2017	23.9984	-98.2705	-	-	-	-	0.00
	05/10/2017	23.9984	-98.2704	-	-	-	-	0.00

Appendix 2. Molarity (M), diffusivity (D), osmotic pressure (π) and ksup

k_{sup} was calculated using *Equation (7)* and the three different values for k_c (10, 14.1 and 50 μm/s). Even though the structural parameter of every membrane is different, it wasn't reported for all the membranes analysed in this work. For this reason, such value was set as the one reported by Field [27]. Loeb's DS data was not included as it was calculated following the procedure explained at section 4.3.2. Molarity was calculated considering a volume of 100L, as stated by [27]. Then, diffusivity was calculated using the molarity values and interpolating them with those reported in [29].

Table 11. Values of salinity, molarity, diffusivity, pressure and mass transfer at the surface layer (k_{sup}) for the different salinity scenarios.

Sample	Salinity (g/kg)	M (mol /L)	D ($\mu m^2/s$)	π (bar)	k_{sup} (μm/s)		
					k_c=10	k_c=14.1	k_c=50
M1	36.3554	0.6207	1473.38	26.97	3.1460	3.4628	4.2041
M4	0.1063	0.0018	1605.55	0.08	3.3342	3.6921	4.5470
P1	34.1592	0.5832	1473.56	25.26	3.1463	3.4631	4.2046
P9	0.2008	0.0034	1599.81	0.14	3.3262	3.6824	4.5323
S1	35.8892	0.6127	1473.42	26.60	3.1461	3.4628	4.2042
S6	0.3300	0.0056	1591.96	0.24	3.3154	3.6691	4.5122
Loeb's FS	29.0438	0.4993	1523.67	4.98	3.1470	3.4640	4.2058
Field 0 M	0.0000	0.0000	1612.00	0.00	3.3430	3.7030	4.5635
Field 0.025 M	1.4644	0.0250	1523.67	1.05	3.2188	3.5512	4.3351
Field 1 M	58.5757	1.0000	1483.00	45.13	3.1600	3.4798	4.2292

Appendix 3. Definitions [14]

Basin: Area of land where water is retained and leads to a river, lagoon, sea or any other kind of water bodies.

Biochemical Oxygen Demand: Analysis used to determine the amount of biodegradable organic matter in a solution.

Consumptive water: Water allocated for a specific activity that would be consumed and, therefore, it can't be completely recuperated after the activity finishes. (I.e. Agriculture, public supply).

Chemical Oxygen Demand: Analysis done to determine the total amount of organic matter in a solution.

Faecal Coliforms: Microorganisms presented mainly in faeces that can be dangerous for humans

Total Suspended Solids: Analysis done to determine the amount of solids that can be retained while filtering a solution using vacuum pressure.

Water Shed: Superficial water enclosed in a delimitated part of land by the landform itself.

Water Stress: Degree of usage of water compared to the amount of renewable water in a specific zone.

Bibliography

[1] SENER, "Balance Nacional de Energia: Produccion de energia primaria (Table)," 2018. [Online]. Available: http://sie.energia.gob.mx/.

[2] “Ley de Transicion Energetica,” Mexico, 2015.

[3] M. Becerra-Perez, "Fuentes de Energia Limpia en Mexico," 1 4 2015. [Online]. Available: https://www.forbes.com.mx/fuentes-de-energia-limpia-en-mexico/.

[4] Estadisticas del Agua en Mexico, Edicion 2017, SEMARNAT, 2017, pp. 49-51.

[5] Estadisticas del Agua en Mexico, Edicion 2017, SEMARNAT, 2017, p. 24.

[6] J. V. Hernandez-Fontes, A. Felix, E. Mendoza, Y. Rodriguez Cueto and R. Silva, “On the Marine Energy Resources of Mexico,” *Journal of Marine Science and Engineering,* 2019.

[7] A. Achilli, T. Y. Cath and A. E. Childress, “Power generation with pressure retarded osmosis: An experimental and theoretical investigation,” *Journal of Membrane Science,* vol. 343, pp. 42-52, 11 2009.

[8] A. Achilli and A. E. Childress, “Pressure retarded osmosis: From the vision of Sidney Loeb to the first prototype installation - Review,” *Desalination,* vol. 261, pp. 205-211, 10 2010.

[9] H. T. Madsen, S. S. Nissen and E. G. Søgaard, “Theoretical framework for energy analysis of hypersaline pressure retarded osmosis,” *Chemical Engineering Science,* vol. 139, pp. 211-220, 1 2016.

[10] A. Altaee and A. Sharif, “Pressure retarded osmosis: advancement in the process applications for power generation and desalination,” *Desalination,* vol. 356, pp. 31-46, 1 2015.

[11] M. Kurihara and H. Takeuchi, “SWRO-PRO System in "Mega-ton Water System" for Energy Reduction and Low Environmental Impact,” *Water,* vol. 10, p. 48, 1 2018.

[12] S. Loeb, “Large-scale power production by pressure-retarded osmosis, using river water and sea water passing through spiral modules,” *Desalination,* vol. 143, pp. 115-122, 5 2002.

[13] K. Gerstandt, K.-V. Peinemann, S. E. Skilhagen, T. Thorsen and T. Holt, “Membrane processes in energy supply for an osmotic power plant,” *Desalination,* vol. 224, pp. 64-70, 4 2008.

[14] Estadisticas del Agua en Mexico, Edicion 2018, SEMARNAT, 2018.

[15] A. Cipollina and G. Micale, Sustainable Energy from Salinity Gradients, Woodhead Publishing, 2016.

[16] T. Thorsen and T. Holt, “The potential for power production from salinity gradients by pressure retarded osmosis,” *Journal of Membrane Science,* vol. 335, pp. 103-110, 6 2009.

[17] A. A. Zavitsas, “Properties of Water Solutions of Electrolytes and Nonelectrolytes,” *The Journal of Physical Chemistry B,* vol. 105, pp. 7805-7817, 8 2001.

[18] E. Brown, A. Colling, D. Park, J. Phillips, D. Rothery and J. Wright, Seawater: Its composition, properties and behaviour., Oxford, UK: Butterworth Heinemann, 1989.

[19] A. S. Civil Engineers, Hydrology handbook, 2nd ed ed., New, York: ASCE, 1996.

[20] C. F. Wan, T. Yang, W. Gai, Y. D. Lee and T.-S. Chung, "Thin-film composite hollow fiber membrane with inorganic salt additives for high mechanical strength and high power density for pressure-retarded osmosis," *Journal of Membrane Science,* vol. 555, pp. 388-397, 6 2018.

[21] Y. Li, S. Zhao, L. Setiawan, L. Zhang and R. Wang, "Integral hollow fiber membrane with chemical cross-linking for pressure retarded osmosis operated in the orientation of active layer facing feed solution," *Journal of Membrane Science,* vol. 550, pp. 163-172, 3 2018.

[22] S. Chou, R. Wang, L. Shi, Q. She, C. Tang and A. G. Fane, "Thin-film composite hollow fiber membranes for pressure retarded osmosis (PRO) process with high power density," *Journal of Membrane Science,* vol. 389, pp. 25-33, 2 2012.

[23] Z. L. Cheng, X. Li, Y. D. Liu and T.-S. Chung, "Robust outer-selective thin-film composite polyethersulfone hollow fiber membranes with low reverse salt flux for renewable salinity-gradient energy generation," *Journal of Membrane Science,* vol. 506, pp. 119-129, 5 2016.

[24] Z. L. Cheng and T.-S. Chung, "Mass transport of various membrane configurations in pressure retarded osmosis (PRO)," *Journal of Membrane Science,* vol. 537, pp. 160-176, 9 2017.

[25] Q. She, R. Wang, A. G. Fane and C. Y. Tang, "Membrane fouling in osmotically driven membrane processes: A review," *Journal of Membrane Science,* vol. 499, pp. 201-233, 2016.

[26] J. J. Wu, "Note on Updating Loeb Analysis for the Effect of Salinity," July 23rd, 2018.

[27] R. W. Field, F. A. Siddiqui, P. Ang and J. J. Wu, "Analysis of the influence of module construction upon forward osmosis performance," *Desalination,* vol. 431, pp. 151-156, 4 2018.

[28] R. Mills, "The effect of the ionization of water on diffusional behavior in dilute aqueous electrolytes," *J. Phys. Chem,* vol. 66, no. 12, pp. 2716-2718, 1962.

[29] R. H. Stokes, "The Diffusion Coefficients of Eight Uni-univalent Electrolytes in Aqueous Solutions at 25°," *J. Am. Chem. Soc.,* vol. 72, no. 5, pp. 2243-2247, 1950.

[30] J. Y. Xiong, Z. L. Cheng, C. F. Wan, S. C. Chen and T.-S. Chung, "Analysis of flux reduction behaviors of PRO hollow fiber membranes: Experiments, mechanisms, and implications," *Journal of Membrane Science,* vol. 505, pp. 1-14, 5 2016.

[31] Y.-N. Wang, E. Järvela, J. Wei, M. Zhang, H. Kyllönen, R. Wang and C.-Y. Tang, "Gypsum scaling and membrane integrity of osmotically driven membranes: The effect of membrane materials and operating conditions," *Desalination,* no. 377, pp. 1-10, 2016.

[32] A. Kumano, K. Marui and Y. Terashima, "Hollow fiber type PRO module and its characteristics," *Desalination,* vol. 389, pp. 149-154, 7 2016.

[33] K. G. Nayar, M. H. Sharqawy, L. D. Banchik and V. John H. Lienhard, “Thermophysical properties of seawater: A review and new correlations that include pressure dependence,” *Desalination,* vol. 390, pp. 1-24, 7 2016.

[34] M. H. Sharqawy, J. H. Lienhard and S. M. Zubair, “Thermophysical properties of seawater: a review of existing correlations and data,” *Desalination and Water Treatment,* vol. 16, pp. 354-380, 4 2010.

[35] K. L. Hickenbottom, J. Vanneste, M. Elimelech and T. Y. Cath, “Assessing the current state of commercially available membranes and spacers for energy production with pressure retarded osmosis,” *Desalination,* vol. 389, pp. 108-118, 7 2016.

[36] M. Tian, Y.-N. Wang, R. Wang and A. G. Fane, “Synthesis and characterization of thin film nanocomposite forward osmosis membranes supported by silica nanoparticle incorporated nanofibrous substrate,” *Desalination,* vol. 401, pp. 142-150, 1 2017.

[37] X. Fan, Y. Liu, X. Quan and S. Chen, “Highly Permeable Thin-Film Composite Forward Osmosis Membrane Based on Carbon Nanotube Hollow Fiber Scaffold with Electrically Enhanced Fouling Resistance,” *Environmental Science & Technology,* vol. 52, pp. 1444-1452, 1 2018.

[38] M. Yasukawa, D. Shigefuji, M. Shibuya, Y. Ikebe, R. Horie and M. Higa, “Effect of DS Concentration on the PRO Performance Using a 5-Inch Scale Cellulose Triacetate-Based Hollow Fiber Membrane Module,” *Membranes,* vol. 8, p. 22, 5 2018.

[39] C. F. Wan, B. Li, T. Yang and T.-S. Chung, “Design and fabrication of inner-selective thin-film composite (TFC) hollow fiber modules for pressure retarded osmosis (PRO),” *Separation and Purification Technology,* vol. 172, pp. 32-42, 1 2017.

[40] Y. Li, S. Qi, Y. Wang, L. Setiawan and R. Wang, “Modification of thin film composite hollow fiber membranes for osmotic energy generation with low organic fouling tendency,” *Desalination,* vol. 424, pp. 131-139, 12 2017.

[41] C. F. Wan and T.-S. Chung, “Energy recovery by pressure retarded osmosis (PRO) in SWRO–PRO integrated processes,” *Applied Energy,* vol. 162, pp. 687-698, 1 2016.

[42] L. Shen, S. Xiong and Y. Wang, “Graphene oxide incorporated thin-film composite membranes for forward osmosis applications,” *Chemical Engineering Science,* vol. 143, pp. 194-205, 4 2016.

[43] L. Huang, J. T. Arena and J. R. McCutcheon, “Surface modified PVDF nanofiber supported thin film composite membranes for forward osmosis,” *Journal of Membrane Science,* vol. 499, pp. 352-360, 2 2016.

[44] R. C. Ong, T.-S. Chung, J. S. Wit and B. J. Helmer, “Novel cellulose ester substrates for high performance flat-sheet thin-film composite (TFC) forward osmosis (FO) membranes,” *Journal of Membrane Science,* vol. 473, pp. 63-71, 1 2015.

[45] A. D. Wilson and F. F. Stewart, “Deriving osmotic pressures of draw solutes used in osmotically driven membrane processes,” *Journal of Membrane Science,* vol. 431, pp. 205-211, 3 2013.

[46] “NMX-AA-051-SCFI-2001 "Water analysis - Measurementes of metals by atomic absorption in natural waters, drinking, wastewaters and treated wastewaters - Test method",” Mexico, 2016.

[47] “NMX-AA-072-SCFI-2001 "Water analysis - Determination of total hardness in natural, wastewaters and wastewaters treated - Test method",” Mexico, 2001.

[48] “NMX-AA-034-SCFI-2016 "Water analysis - Measurement of salts and solids dissolved in natural waters, drinking, wastewaters and treated wastewaters - Test method",” Mexico, 2016.

[49] “NMX-AA-007-SCFI-2016 "Water analysis - Determination of temperature in natural waters, drinking, wastewaters and treated wastewaters - Test method",” Mexico, 2013.

[50] S. Zhang, P. Sukitpaneenit and T.-S. Chung, “Design of robust hollow fiber membranes with high power density for osmotic energy production,” *Chemical Engineering Journal,* vol. 241, pp. 457-465, 4 2014.

[51] P. Sukitpaneenit and T.-S. Chung, “High Performance Thin-Film Composite Forward Osmosis Hollow Fiber Membranes with Macrovoid-Free and Highly Porous Structure for Sustainable Water Production,” *Environmental Science & Technology,* vol. 46, pp. 7358-7365, 6 2012.